University of Natural Resources and Life Sciences, Vienna

Department of Biotechnology

(Head: Ao.Univ.Prof. Dipl.-Ing. Dr.nat.techn. Florian Rüker)

Clarification of *E. coli* homogenates by precipitation

Masterarbeit

zur Erlangung des akademischen Grades

Diplom-Ingenieur

Verfasst von Mathias Fink, BSc.

Vorstand: Ao.Univ.Prof. Dipl.-Ing. Dr.nat.techn. Florian Rüker
Betreuer: Assoc. Prof. Dipl.-Ing. Dr.nat.techn. Rainer Hahn
Mitbetreuer: Dipl.-Ing. Dr.nat.techn. Markus Luchner

Eidesstattliche Erklärung

Ich erkläre ehrenwörtlich, dass ich die vorliegende Arbeit selbständig und ohne fremde Hilfe verfasst habe, nicht andere als die angegebenen Quellen verwendet habe und die benutzten Quellen wörtlich oder inhaltlich entnommenen Stellen als solche kenntlich gemacht habe

Reichenau an der Rax,_____ _____
Datum Unterschrift

Statutory declaration

I declare that I have authored this thesis independently, that I have not used other than the declared sources and that I have explicitly marked all material, quoted either literally or by content from the used sources.

Reichenau an der Rax,_____ _____
Date Signature

Danksagung

Die Möglichkeit zu bekommen meine Diplomarbeit an der Pilotplant der Universität für Bodenkultur machen zu können, war für mich eine große Ehre und eine einmalige Gelegenheit. Das Projekt, das mit der Gestaltung dieser einzigartigen Anlage verwirklicht wurde ist atemberaubend und zeigt was durch großen Einsatz im universitären Umfeld möglich ist. Die Möglichkeit an der Universität im Pilotmaßstab und GMP nahem Umfeld im Laufe von Studentenübungen und Abschlussarbeiten tätig sein zu können ist sehr zu schätzen und von großem Wert für die berufliche Laufbahn.

Ich möchte mich bei einigen Personen die mich während meiner Diplomarbeit begleitet haben recht herzlichst bedanken. Beginnend bei Sabine Necina, die mir insbesondere am Anfang meiner Arbeit tatkräftig unter die Arme gegriffen hat und mich bei der Planung und Durchführung meiner Versuche sehr unterstützt hat. Auch während der restlichen Zeit meiner Arbeit stand sie mir immer mit Rat und Tat zur Seite wenn ich nicht weiter wusste und hatte immer ein offenes Ohr für mich. Danke dafür.

Auch Clemens Keinprecht gebührt Dank dafür dass er mich unterstützte wo er konnte und mir auch im Bereich der Fermentation vieles gezeigt und erklärt hat. Er war immer sehr bemüht mir bei Problemen die im Alltag auftauchten zu helfen. Auch privat lernte ich ihn sehr zu schätzen.

Weiters möchte ich meinem Kollegen Bernhard Sissolak danken. Er unterstützte mich während meiner gesamten Zeit in der Pilotplant und stand mir bei praktischen und theoretischen Fragen immer kompetent zur Seite. Selbst wenn er wegen seiner eigenen Diplomarbeit viel zu tun hatte konnte ich immer mit meinen Fragen zu ihm kommen. Er erklärte mir die benötigten Messverfahren und Auswertungen und so konnte ich von ihm sehr vieles lernen. Außerdem sorgte er immer für ein sehr angenehmes und lockeres Arbeitsumfeld.

Allen anderen aus der Arbeitsgruppe möchte ich dafür danken, dass ich so gut aufgenommen worden bin und für jegliche Hilfe die ich von ihnen bekommen habe.

Schließlich möchte ich noch meinen beiden Betreuern Rainer Hahn und Markus Luchner danken. Sie haben diese einzigartige Gelegenheit für mich erst möglich gemacht. Danke dafür, dass ihr mich so gut betreut habt, sowohl fachlich als auch menschlich war ich stets begeistert von euch. Während meiner gesamten Zeit bei euch seit ihr mir jederzeit mit Rat und Tat zur Seite gestanden, habt mir meine Fragen beantwortet und gezeigt wie ich die auftretenden Herausforderungen meistere. Außerdem habt ihr mir den Freiraum gelassen selbständig zu arbeiten und mich selbst zu organisieren. Für all das bin ich euch zu sehr großem Dank verpflichtet. Ich habe während meiner Zeit bei euch sehr vieles lernen können.

Das gesamte Pilotplant Team ist mir während meiner Zeit mit ihnen sehr ans Herz gewachsen und sie haben die Zeit für mich unvergesslich gemacht und mir gleichzeitig sehr viel für meinen weiteren Lebensweg mitgegeben. Danke vielmals an euch.

Abstract

The biotechnological production of recombinant proteins is widespread used and an important industrial branch for example in the pharmaceutical production of recombinant insulin, erythropoietin or antibodies.

Escherichia coli is one of the dominating microorganisms in the production of recombinant proteins. It has a long tradition and is one of the best investigated and most often used model organisms for research and production in the field of biotechnology and molecular biology. Although research is performed with other organisms and it is not able to perform post translational modifications such as glycosylation it is still one of the most often used production hosts. The fermentation process is well studied, fast and comparatively cheap.

In the course of this thesis downstream processing of green fluorescent protein (GFP) produced in the *E. coli* strain HMS 174(DE3) with the plasmid pET11a-GFPmut3.1 was investigated in detail. GFP is used as model protein as it is easy detectable by eye in the fermentation broth using a handheld UV-lamp and subsequently, it is detectable and quantifiable easily in suspension after each unit operation. For the release of the intracellular product high pressure homogenization was used.

During the purification of GFP it occurred that a precipitate was formed over time in the suspensions, even after centrifugation and filtration. This precipitation event complicated the downstream process as it resulted in bad filtration performance, repetitive filtration steps and the risk of damaging chromatography columns. Furthermore, a massive displacement effect was observable during ion exchange chromatography (IEX) at high feed concentrations, which was thought to be caused by the same compounds inducing precipitation. So the first part of this thesis was the characterization of this precipitate and to determine why and under which conditions precipitation starts. As it was shown that the precipitate consists of a high amount of protein and its formation was mainly influenced by storage temperature, the next step was to introduce a selective precipitation step.

Heat, $CaCl_2$ and poly ethylene glycol (PEG) were used as precipitating agents. As both $CaCl_2$ and PEG resulted in relatively high product losses, those are not capable as purification step after homogenization. For heat precipitation it was shown that the best results regarding clearance efficiency, purification effect and product yield were reached when the unclarified homogenate was treated for 3 hours at 50 °C and clarified by centrifugation afterwards.

The adsorption performance was investigated with the anion exchange resins CaptoQ and Q-Sepharose FF. After heat treatment the displacement effect was still observable although much less effective and occurred mainly at higher feed and thus protein concentrations.

Furthermore, it was investigated how host DNA was influenced by homogenization conditions and it was shown that increasing number of stages and passages of homogenization resulted in smaller DNA fragments.

Contents

List of figures

List of tables

Abbreviations

bp ..... Base pair
BRET ..... Bioluminiscence resonance energy transfer
BSA ..... Bovine serum albumin
CDM ..... Cell dry mass
CV ..... Column volume
DAD ..... Diode array detector
DF ..... Dia filtration
ds ..... Double stranded
EGFP ..... Enhanced Green Fluorescent Protein
FRET ..... Fluorescence resonance energy transfer
GFP ..... Green Fluorescent Protein
HETP ..... Height equivalent to a theoretical plate
HIC ..... Hydrophobic interaction chromatography
HPLC ..... High pressure liquid chromatography
IEX ..... Ion exchange chromatography
Ig ..... Immunoglobulin
IPTG ..... Isopropyl β-D-1-thiogalactopyranoside
PBS ..... Phosphate buffered saline
PEG ..... Poly ethylene glycol, Poly ethylene glycol
pI ..... Isoelectric point
rpm ..... Rounds per minute
SDS-PAGE ..... Sodium dodecyl sulfate poly acrylamide gel electophoresis
SEC ..... Size exclusion chromatography
UF ..... Ultra filtration

1 Introduction

1.1 The green fluorescent protein (GFP)

1.1.1 Discovery and applications of GFP

The discovery and investigation of GFP was primarily embossed by three scientists, Osamu Shimomura, Martin Chalfie and Roger Tsien who were awarded the Nobel Prize in Chemistry in 2008 for their basic research on GFP (Sanders & Jackson 2009). The bioluminescence of *Aequorea victoria* was discovered by Davenport and Nicol in 1955, it was identified to be caused by GFP by Shimomura et al. in the early 1960s*. In vivo* the fluorescence of GFP is dependent on the interaction of aequorin with Ca^{2+} ions, which leads to the excitation of its chromophore and emission of blue light by relaxation to its groundstate. Due to this relaxation, energy is transferred radiationless to GFP and green light is emitted, the same effect was observed in the hydrozoa *Obelia* and the sea pen *Renilla* by Morin and Hastings (Roda 2010).

Figure 1: Aequorea victoria (Shimomura 2005).

This kind of energy transfer is called Förster-type energy transfer. Morize et al. purified and crystallized GFP in 1974 this work allowed the elucidation of GFP's chromophore structure by Shimomura in 1979 (Shimomura 2005). Martin Chalfie was the first to realize the potential that GFP could have for molecular biology as fluorescent *in vivo* marker. After the nucleotide sequence of wild-type GFP was identified and cloned by Douglas Prasher in 1992, he was the one to manage the expression of GFP's coding sequence in *E. coli* and *C. elegans* in 1994. The utilization of wild-type GFP as an analytical tool had some drawbacks and limitations such as poor fluorescence quantum yield or pH and chloride sensitivity. These drawbacks were started to be improved by Roger Tsien who engineered the wild-type resulting in improved thermo stability and different emission wavelengths in 1995. Subsequently, the enhanced GFP (EGFP), blue, cyan and yellow fluorescent mutants were engineered (Roda 2010).

Applications of GFP can be grouped in two main categories, passive applications and as an active indicator. In passive applications it is used either as a tagging agent by fusion tag or as a reporter gene or cell marker. The first time GFP was used as a reporter gene was in *Caenorhabditis elegans*, where gene expression was detected *in vivo*. Furthermore, it can be used for evaluation of gene transfer in transgenic organisms.

As quite strong promoters are required for expression, mostly constitutive promoters from viruses or strong exogenous regulators are used. When GFP is used as a genetic fusion partner, it is possible to observe localization and fate of the tagged host proteins, and even cell organelles can be marked. The fusion proteins keep their native functions and localizations but have the additional function of fluorescence after fusion (Tsien 1998). GFP and its variants are also used as fluorescence reporter donor and acceptor pairs in fluorescence resonance energy transfer (FRET) and bioluminescence resonance energy transfer (BRET). The latter one was directly resulting from the GFP discovery, as GFP is excited by resonance energy transfer from aequorin in *A. victoria.* Furthermore, it is possible to visualize cells in intact whole experimental animals by labeling them with GFP which is a useful instrument for the investigation of cancer growth, metastasis development and effect of drugs (Roda 2010). Owing to recombinant GFP's thermo stability, its application as fluorescent biologic indicator for the efficacy of moist heat treatment below 100 °C is investigated (Vessoni Penna et al. 2004)

Due to its easy detection it also can be used as a model protein for protein purification, as done during this thesis.

1.1.2 Properties of GFP

GFP is a barrel-shaped protein with a molecular mass of approximately 28 kDa and 238 amino acid residues. The barrel is built from 11 antiparallel β-sheets which are connected with α-helical stretches, of which one is spanned through the β-can and forms the fluorescent chromophore (Nagy 2004). Shimomura was the first to postulate that the chromophore is a 4-(*p*-hydroxybenzylidene)imidazolidin-5-one, which is attached to the peptide backbone by the ring's 1 and 2 positions, in 1970 (Roda 2010). The fluorescence of GFP is caused by this intrinsic chromophore which is formed by cyclization and subsequent dehydration and oxidation of the tripeptide Ser65, Tyr66, and Gly67. This formation process is not dependent on any cofactors (Wang et al. 2010). The structure of the chromophore and its position within GFP is shown in Figure 2 .

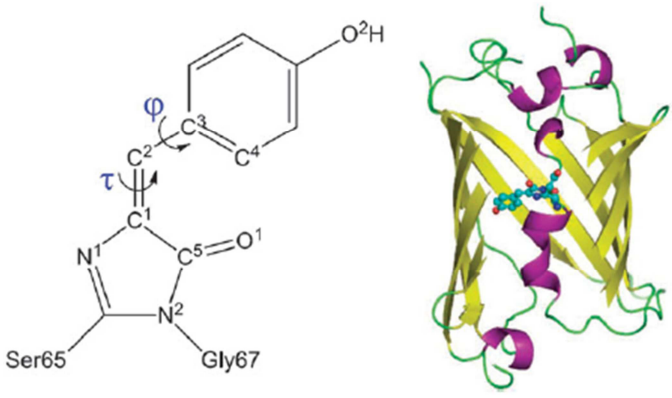

Figure 2:Structure of GFP's chromophore and its location in the protein structure (Wang et al. 2010)

Depending on chromophores' distinctive component GFP variants are divided into seven classes differing in excitation and emission maxima. In class 1, there is the wild-type GFP which has two excitation peaks, one at 395 nm, which has about three times the amplitude of the second peak at 475 nm, resulting in emission peaks at 508 and 503 nm respectively. When wild-type GFP is expressed at or below room temperature folding efficiency is quite good but decreases at higher temperatures. When folded under these conditions it is stable and fluorescent at least up to 65 °C. Wild-type GFP was engineered by DNA shuffling to improve its folding efficiency at 37 °C, reduce aggregation at high concentrations and to increase its duffusibility inside cells. Although it is stable at 65°C excitation at 395 nm

decreases and increases at 470 nm and at 78 °C 50 % of fluorescence is lost due to denaturation (Tsien 1998). Additionally, the process of denaturation by heat is reversible at low temperature (Nagy 2004).

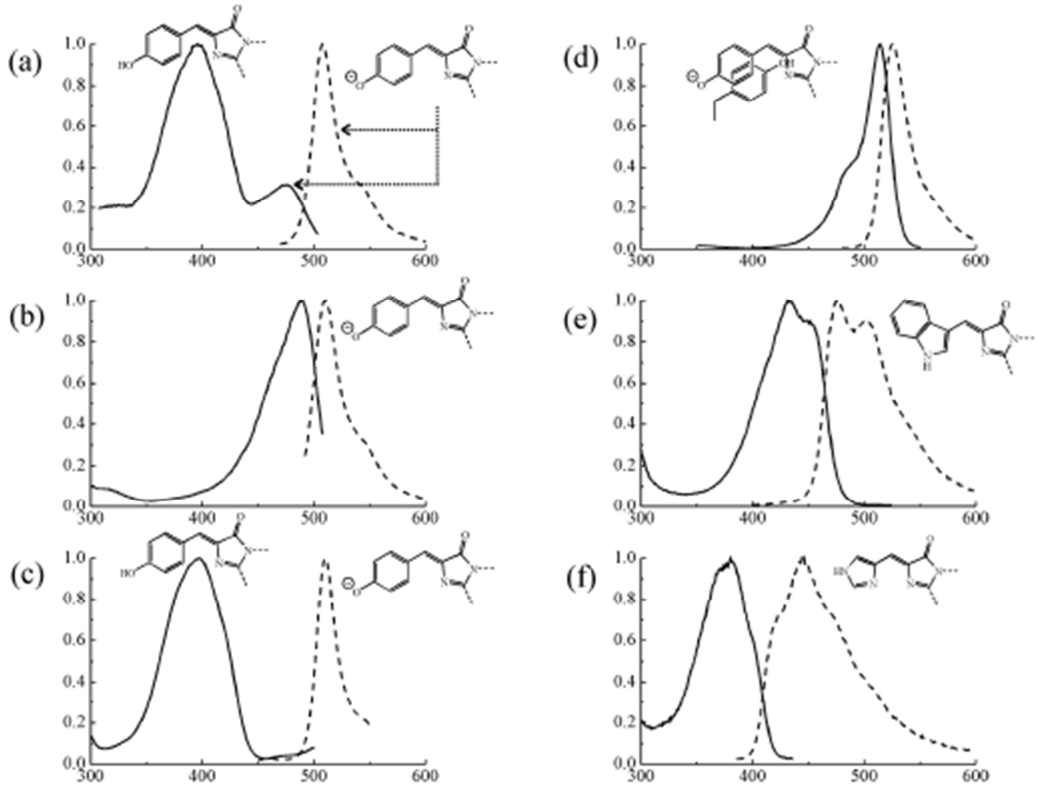

Figure 3: Chromophore structures, as well as fluorescence and emission spectra for six major classes of GFP mutants, depicted by solid and dashed lines respectively. a) wild-type; b) Emerald; c) H9-40; d) Topaz; e) W1B; f) P4-3 (Tsien 1998).

In 2005 it was shown, that the denaturation of GFP by heat and subsequent renaturation is pH dependent. Denaturation at 70 °C was fastest at a pH of 6.5 followed by 7.5 and 8.5 with renaturation performance ranked vice versa. Thus it seems that GFP changes its stability in this pH range with the highest sensitivity at pH 6.5 (Alkaabi et al. 2005). Fluorescence is also affected by pH. At high pH values of 11-12 for example excitation at 395 nm is decreased and increased at 470 nm. The pK_a of wild-type GFP is near to 4.5 which results in quenching by acidic pH. As well as temperature tolerance, pK_as are altered by mutations of GFP (Tsien 1998).

1.2 *Escherichia coli* as host organism

In nature *E. coli* is a very important organism, its native habitat is the lower gut of animals but it survives being released to the environment, as it is facultative anaerobe. This fact results in the possibility to spread to new hosts. Furthermore, there are pathogenic strains that infect the enteric, urinary, pulmonary and nervous systems. However it evolved to be a famous model organism for biochemical genetics, molecular biology and biotechnology, hence it was the earliest candidate for whole genome sequencing and its 4.6 million bp genome was finally published in 1997 (Blattner et al. 1997).

Nowadays, *E. coli* still plays a major role in the production of recombinant proteins and is the most commonly used organism. Because on the one hand its physiological and metabolic characteristics are studied very well and on the other hand laboratories and industry can look back on a long safe use. Somatostatin was the first recombinant human protein that was produced by *E. coli,* followed by insulin in 1982 (Overton 2014).The next milestone was the

production of bovine growth hormone in 1994 (Swartz 2001). Of today's recombinant biologic products approximately 30 % are produced in *E. coli*. For enabling recombinant protein production processes expression vectors that are cloned to the host organism are necessary. Some of the most commonly used promoter systems in *E. coli* are:

- pET system (DE3/T7)
- lac systems (Plac, PlacUVS)
- tac/trc
- pBAD
- λ p_L

Using the pET system, a recombinant plasmid containing the gene for T7 RNA polymerase is transferred to *E. coli* at its DE3 locus. The RNA polymerase is controlled by the lacUV5 promoter, which is inducible by isopropyl β-*D*-1-thiogalactopyranoside (IPTG). When no IPTG is present, the *lac* promoter is bound by the Lac repressor LacI, transcription is repressed and so T7 RNA polymerase is not synthesized. When IPTG is present, the *lac* promoter is no longer bound by LacI and transcription and translation of the T7 RNA polymerase gene is performed. Now the T7 RNA polymerase can get active and the recombinant gene of interest is transcribed (Overton 2014). This system is sketched in Figure 4.

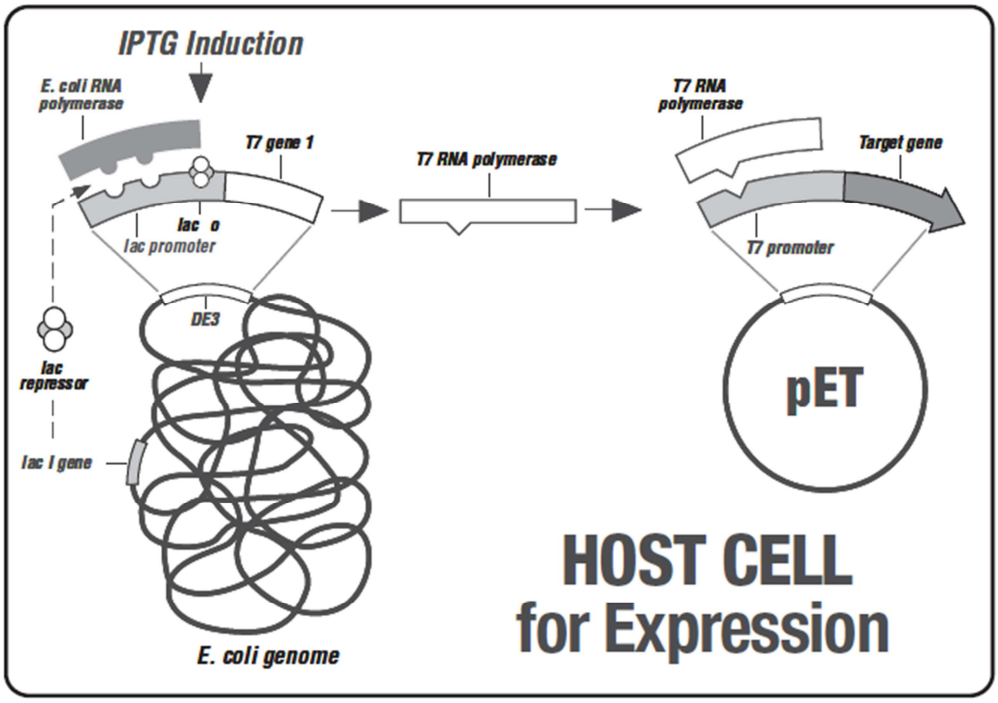

Figure 4: Schematic overview of the functionality of the pET promoter system (Novagen 2003).

1.3 Homogenization theory

As many products of biotechnological fermentation are intracellular, these products have to be released from the cells before following unit operations can be performed for the purification of the product. One operation for this means is high pressure homogenization. The pressure applying valve is shown in Figure 5.

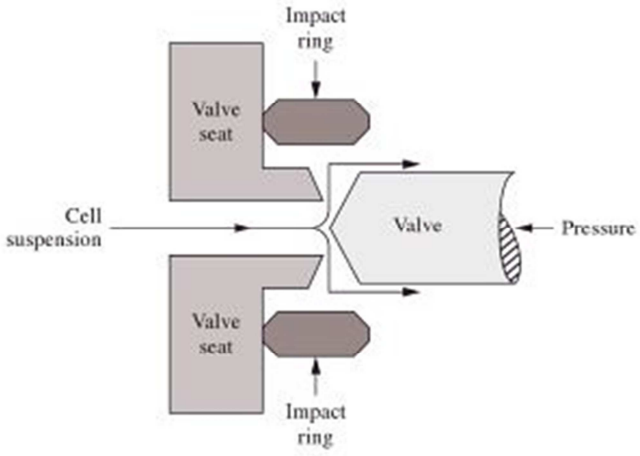

Figure 5: Diagram of the valve region of high pressure homogenizers (Doran 2013).

The cell suspension is pumped through the homogenizer valve at a constant volumetric flow rate by a positive displacement pump. During homogenization process the suspension is accelerated into the gap space between the valve and the valve seat, and then it is decelerated at the impact ring before leaving the homogenizer. The adjustable operating value is the gap space by which the pressure is varied, increasing the applied pressure by decreasing the gap space. Cell breakage is attained by a range of hydrodynamic forces, such as channel inlet pressure gradient, channel shear stress, post channel turbulence and impact ring impingement forces. Although higher pressure results in higher grade of cell breakage there are also adverse effects that go along with increasing pressure, such as thermal degradation caused by heating during homogenization and size reduction of cell debris which can deteriorate following downstream unit operations. Additionally, large product molecules can be destructed by hydrodynamic forces (Kelly & Muske 2004). In the case of soluble intracellular products it is desirable to have high levels of product release coupled with large debris as these are removable better by centrifugation (Wong et al. 1997).

The degree of cell disruption is influenced by the operating conditions and is given by equation 1.1.

$$\ln\left(\frac{R_{max}}{R_{max}-R}\right) = kNp^{\alpha} \qquad 1.1$$

Where R_{max} is the maximum releasable protein, R is the released protein after N passages, k is a temperature dependent constant, p is the operating pressure and α gives the resistance of the cells to disruption, with values between 0.9 and 2.9 for bacteria and yeast. However, k and α are depending on the cell type. Because α is depending on the cell wall's strength there is also given a correlation to the fermentation conditions that influence the growth of the organisms (Doran 2013).

1.4 Precipitation theory

In general, there are some parameters that influence the precipitation performance. These are the nature and concentration of the protein, the type of precipitant, other components in the solution, temperature, pH and Ionic strength of the solution. Separation of precipitates can be performed by filtration, microfiltration or centrifugation but depends on its properties in terms of particle size, size distribution, density and mechanical strength. As filtration and centrifugation are more effective with larger particles it is desirable to reach large precipitate particles. Properties like particle size less than 1 µm, low density differences and colloidal or

gelatinous precipitates complicate particle separation. Precipitation is most often performed in stirred tank batch reactors as the added precipitates need to be mixed well.

Precipitate formation is a three step procedure including nucleation, growth and aging. It starts with nucleation, the formation of submicron-sized particles which can occur very quickly, which makes it essential to mix the solution well to distribute the precipitant and to ensure as homogenous precipitates as possible. The more rapid the nucleation takes place, the more important it is to mix well. The growth phase initially depends on diffusion processes with solute molecules nearby the nuclei, diffusing to the particles. Furthermore, it is promoted by mixing, as particles collide and are forming agglomerates. However, mixing speed has to be evaluated well as too high shear rates result in smaller particles. During aging the particles still grow in size but also improve stability and density. At this stage less intense mixing is required.

Precipitation methods include salting out by high salt concentrations, disrupting the hydration barriers between protein molecules, isoelectric precipitation, weakening the electrical double layer around soluble proteins, consequently decreasing the electrostatic repulsion between nearby proteins. Moreover, it is possible to perform precipitation with organic solvents that are water soluble and weakly polar, like ethanol or acetone, according to their lower dielectric constant, the attraction between polar groups gets stronger and proteins aggregate due to greater attractive forces of their oppositely charged groups. Additionally, the hydration level of globular proteins is decreased by organic solvents. Another method is the precipitation with nonionic water soluble polymers like poly ethylene glycol (PEG). The higher the molecular masses of proteins, the lower PEG concentrations are needed. Its effect is similar to that of organic solvents (Doran 2013). PEG for instance is used as precipitating agent during purification of antibodies to improve chromatography performance (Giese et al. 2013) or in combination with $CaCl_2$ to develop a direct capture step during purification of recombinant antibodies. The combination is exploiting the precipitation of high molecular mass impurities, like dsDNA and aggregates by $CaCl_2$, and the separation of low molecular mass impurities such as host cell proteins by PEG (Sommer et al. 2014).

Another precipitation practice that is used as preliminary purification step, for example for treatment of unclarified *E. coli* homogenates, is heat treatment. This operational step results in precipitation and denaturation of heat labile host proteins and thermal deactivation of host proteases. Ng et al. used this approach during purification of recombinant hepatitis B core antigen from unclarified *E. coli* homogenate. Their experiments showed that product recovery yield and purity were evidently increased by heat treatment at 60 °C for 45 minutes, compared to not heat treated material. After heat treatment the feedstocks were gradually cooled down to room temperature (Ng et al. 2006).

1.5 Ion Exchange Chromatography (IEX)

1.5.1 General

Due to their structure, containing acidic and basic amino acids as well as amino and carboxyl termini at their polypeptide chains, proteins have positive and negative charges and are therefore amphoteric molecules. The more acidic proteins are, the higher is their negative charge. The number of ionizable amino acid residues and their pK_a values determine the net charge of a protein. The pH of the protein's environment is affecting its net charge, as the protonation of ionizable amino acid residues change with pH, depending on their pK_a values. When the pH value is two units higher than the pK_a, acidic residues are completely deprotonated and thus negatively charged. At pH values two units below the pK_a of basic residues, they are completely protonated and thus positively charged. When the isoelectric point (pI) of proteins is reached at a particular pH, their net charge becomes zero (Carta &

Jungbauer 2010). Exactly this net surface charge is utilized by IEX and as the relationship between net charge and pH is unique for each protein it can be used to separate them. During IEX, binding and elution of proteins is performed by reversible interactions between the charged IEX resin and charged molecules. Due to their described properties proteins bind to positively charged anion exchangers if the pH is above its pI conversely they bind to negatively charged cation exchangers at pH values below its pI (GE Healthcare 2004).

During this thesis the anion exchange resins Q Sepharose Fast Flow and CaptoQ were used. Both are strong anion exchange resins with quaternary amine groups ($-N^{+}(CH_3)_3$). CaptoQ has a highly cross-linked agarose matrix with dextran surface extender, which results in higher capacities and mass transfer properties. This brings the benefit of high dynamic binding capacity, due to fast mass transfer. Additionally, shorter overall processing time could be caused by higher binding capacity, as total cycle number may be reduced. A comparison of the dynamic binding capacity of those resins is shown in Figure 6 (GE Healthcare 2015). Q Sepharose's matrix is made out of 6% agarose chains that are arranged in bundles with different degrees of intra-chain cross linking resulting in a range of rigid and macroporous matrices with good capacity and low non-specific adsorption (GE Healthcare 2004).

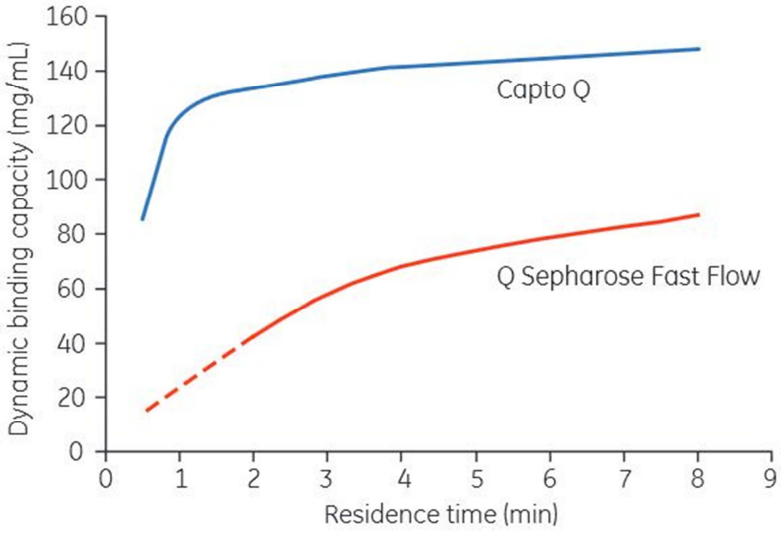

Figure 6: Comparison of dynamic binding capacity as a function of residence time for CaptoQ and Q Sepharose Fast Flow. Bound protein was bovine serum albumin (BSA). For Sepharose dashed lines are used below a residence time of two minutes, as shorter residence times are not possible in large-scale columns with this resin (GE Healthcare 2015).

During the investigation of ion exchangers another huge progress was reached by the development of monoliths as chromatography material. These can be used for separation of large biomolecules, with the advance that fast operation is possible and high capacity for large biomolecules is given. The fast operation is enabled because the height equivalent to a theoretical plate (HETP) and dynamic binding capacity are stable over velocity changes. Examples for separable proteins using monolithic ion exchange columns are blood coagulation factor VII, IgM from serum or monoclonal IgM from cell culture (Jungbauer & Hahn 2008).

1.5.2 Adsorption isotherms

In the presence of highly selective adsorbents, when the adsorption equilibrium is linear or when very small amounts of impurities are present, it is possible to consider a system as single component system. An adsorption isotherm expresses the concentration of a protein that is adsorbed by the stationary phase at equilibrium with the mobile phase. The

equilibrium in a low concentration range is expected to show a linear relationship but mostly it is nonlinear when high protein concentrations are used and if the system is close to the maximum capacity. However, the linear limit is subject to the concentration of accessible binding sites and the specific affinity of the protein to these sites, whereas the accessible surface area and the concentration of binding sites influence the maximum capacity. Adsorption isotherms are obtained at constant mobile phase composition, as protein adsorption is affected by temperature and the composition of the mobile phase. Especially ion-exchange is very sensitive to its composition. IEX is optimally performed at low salt concentrations, as at high salt concentrations the isotherm becomes shallower which is also indicated in Figure 7.

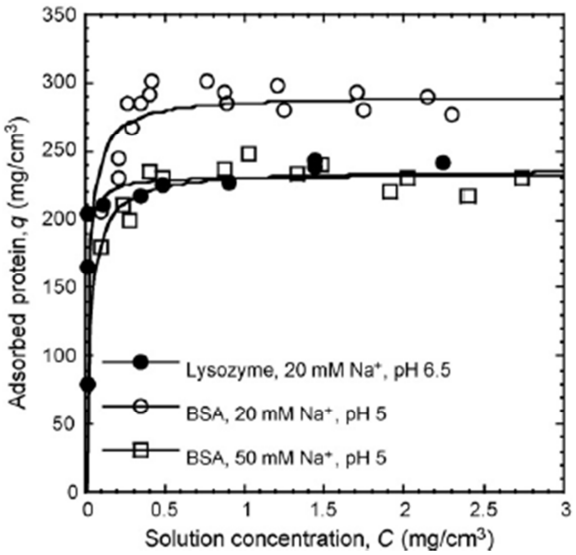

Figure 7: Adsorption isotherms for Lysozyme and BSA at different sodium acetate concentrations for SP-Sepharose-FF (Stone & Carta 2007).

The Langmuir isotherm is a model that is used to describe protein adsorption equilibrium and is calculated by the following equation. Where q is the adsorbed concentration in mg protein per mL resin, q_m is the maximum adsorption capacity, K the equilibrium constant and C the concentration in the supernatant.

$$q = \frac{q_m K C}{1 + K C} \tag{1.2}$$

The Langmuir isotherm can also be expressed in terms of the dimensionless separation factor R for process application.

$$R = \frac{1}{K C_{ref}} \tag{1.3}$$

Where the feed or initial values are taken as reference concentration C_{ref}.

However, in practice multi-component systems, such as fermentation broths are used. They represent a mixture of many different components and protein products can be highly heterogeneous due to post translational modifications. It is possible to describe those complex systems as a three component system with one component being defined as all compounds with lower affinity to the resin material than the product, one component being the product and the third component including all compounds with a higher affinity. The extended Langmuir isotherm for multi component systems with different values of q_m for different components N is given as follows (Carta & Jungbauer 2010).

$$q_i = \frac{q_{m,i} K_i C_i}{1 + \sum_{j=1}^{N} K_j C_j} \tag{1.4}$$

1.6 Currently used recombinant GFP purification procedure in pilot scale

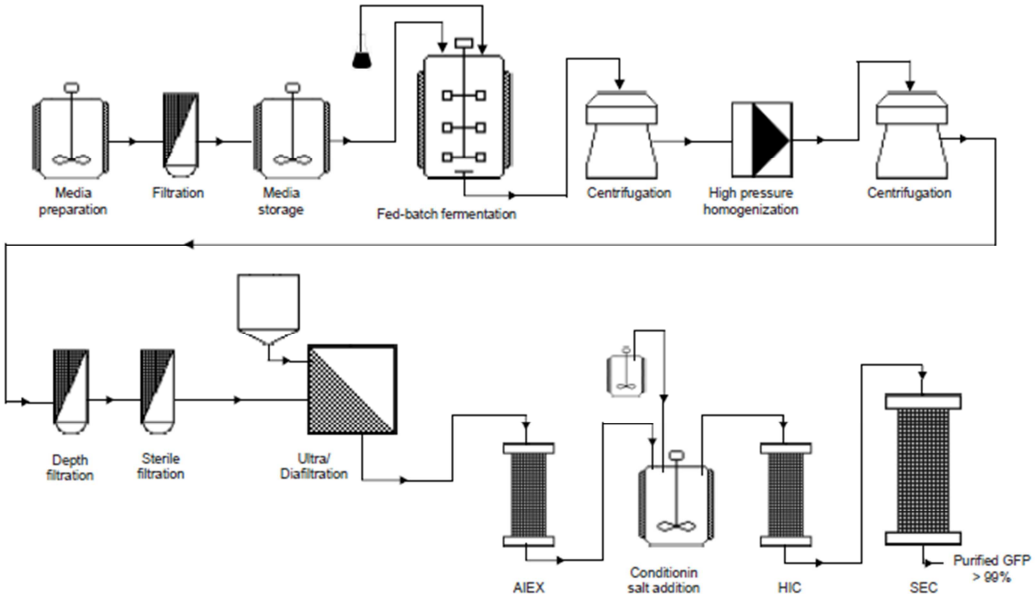

Figure 8: Process diagram of GFP production and purification (Hahn & Luchner 2015).

The currently used purification of GFP from *E. coli* fermentation broth is shown schematically in Figure 8 and is performed as follows. The first step after fermentation is the cell harvest. This operational step is performed with a disk stack centrifuge at 13625 rpm, with a flow rate of 60 L/h. This pellet is resuspended in a homogenization buffer composed of 10 mM Tris, 100 mM NaCl, 0.1 % Tween 20 and adjusted to a pH of 7.5 by 25 % HCl, which is chilled to +4 °C in advance. The cell suspension is prepared with a final cell density of 25 $\frac{gCDM}{L}$. This cell suspension is homogenized with a two stage high pressure homogenizer at 700 and 70 bar, first and second stage respectively for two passages, with a flow rate of 100 L/h in order to perform cell disruption. For cell debris removal again a disk stack centrifuge at 13625 rpm, with a flow rate of 30 L/h is used. Preliminary filtration tests are necessarily performed with the filtration test device to determine the required filter for depth and sterile filtration. For the next step the Sartoflow® Advanced UF/DF device equipped with a Hydrosart® membrane with a molecular weight cut-off of 10 kDa and an area of 0.6 m² is used. During this operational step the buffer is exchanged to a 10 mM Tris/HCl buffer within 5 volume changes and the suspension is concentrated if necessary.

IEX is the first chromatography step. It is performed with Q-Sepharose FF resin, which is packed in an Axichrom 100/300 column with a bed height of approximately 16 cm. As running buffer (buffer A) a 10 mM Tris/HCl buffer at pH 7.5 is used, the elution buffer (buffer B) is a 10 mM Tris, 1 M NaCl buffer at pH 7.5. The applied residence time is 4 min. after which a gradient elution with three steps - 5 % buffer B 3 CV, 30 % buffer B 3 CV and 100 % buffer B 5 CV – is performed.

Before the IEX eluate is loaded to the hydrophobic interaction chromatography (HIC) column, its salt concentration has to be increased to a final concentration of 3.3 M NaCl by addition of a 4.5 M NaCl solution. For HIC the Butyl Sepharose HP resin is used in a Sepacor 90/300 column with a bed height of approximately 15 cm. The sample is loaded to the column with a velocity of 100 cm/h, washed with 1 CV of buffer B and eluted by a three step gradient with 2

CV 20 %, 3 CV 80 % and finally 3 CV 100 % buffer A. Buffer B now is the running buffer with 10 mM Tris and 3.3 M NaCl at pH 7.5.

The polishing step is performed by size exclusion chromatography (SEC). Superdex 75 resin is packed in an Axichrom 100/500 column to reach a bed height of approximately 40cm. The sample loading volume is about 3 % of the column volume, which is achieved by a velocity of 30 cm/h. As running buffer phosphate buffered saline (PBS) is used.

Finally the purified GFP is analyzed by HPLC with an Agilent BIOSEC5 5 µm 300 Å column at a flow rate of 0.3 mg/mL. The measured spectrum is recorded by a diode array detector (DAD). The purity is determined by the 280:490 ratio which is measured with a photometer.

1.7 Master's thesis objectives

During the purification of GFP from E. coli homogenate a precipitation is taking place repeatedly. Even after centrifugation and filtration this phenomenon is appearing. This leads to adverse filtration behavior and the risk of destructing chromatography columns, as precipitation could take place inside those. Additionally, these compounds may be the reason for displacement effects going on during AIEX.

In order to eliminate this phenomenon, the following questions have been tried to answer during the practical work of this master's thesis.

- What is the precipitate composed of?
- Is the precipitate soluble?
- Does it contain DNA?
- Under which conditions does precipitation occur?
- Is it possible to precipitate the substances selectively?
- Is the precipitation depending on the buffer composition?
- Does the substance have impact on the ion exchange chromatography?

2 Material and Methods

2.1 Material and devices

Table 1: List of used materials.

Unit operation	Material / Chemical	Lot-No. / Order No.	Company
IEX	CaptoQ	10070381 / 17-5316-03	GE Healthcare
Analytics	Mini-Protean® TGX™ precast polyacrylamide Gels	/ # 456-1095	Bio-Rad Laboratories, Inc.
IEX	Q-Sepharose FF	10021699 / 17-0510-04	GE Healthcare
Misc.	TRIS Pufferan 99,9 % p.a.	233196559 / 4855.300	Carl Roth GmbH + Co. KG
Misc.	Tween® 20 Polyethylene glycol sorbitan monolaurate	SZBD2190V / P1379-1L	Sigma-Aldrich Co.

Analytics	Quant-iT™ Protein Assay Kit	/ Q33210	Invitrogen
Analytics	Precision Plus Protein™ Dual Color Standard	#161-0374	Bio-Rad Laboratories, Inc.
Purification	Benzonase® Nuclease	/ 70664-3	Novagen®
Analytics	10 x TGS Running Buffer	/ #161-0772	Bio-Rad Laboratories, Inc.
Analytics	4 x Laemmli Sample Buffer	/ # 161-0747	Bio-Rad Laboratories, Inc.
Purification	Poly ethylene glycol 6000		Fluka Biochemicals

Table 2: List of used devices.

Unit operation	Device	Serial No. / Inventory No.	Company
Analytics	Carry 60 UV-Vis G6860A	MY13480019 / 1682	Agilent Technologies
Centrifugation	Centrifuge 415R	/ 1124	Eppendorf
Centrifugation	Disc stack centrifuge PCS 1	1729 / 791	GEA westfalia separation Technology GmbH
Centrifugation	Heraeus Contifuge Stratos Centrifuge	41576127	Thermo Fisher Scientific
Homogenization	Homogenizator Panda	8204	GEA Niro Soavi
Analytics	Infinite M200Pro	1305004737 / 1514	Tecan
Centrifugation	Lab centrifuge Sigma 2-16P	122109 / 095723	Sigma
Analytics	Mini-Protean® Tetra System	552BR 113608 / #165-8037	Bio-Rad Laboratories, Inc.
Analytics	Portable Turbidimeter 2100Q	13100C028466	HACH
Analytics	PowerPac™ Basic	041BR114202 / #164-5050	Bio-Rad Laboratories, Inc.
Analytics	Precision Cells SUPRASIL 10 mm	104.002-QS	Hellma
Mixing	Rotator SB3	R110002435	Stuart
Heating	HAAKE F8	57831-2 / -	Artisan Technology Group
Analytics	AC 121 S		Sartorius

2.2 Methods

2.2.1 Fermentation

For the production of recombinant GFP the *E. coli* strain HMS174(DE3) carrying the pET11a GFPmut3.1 plasmid with an ampicillin resistance marker was used. The used operating procedure for fermentation was a fed-batch culture at 37 °C, pH 7 and a pO_2 of 30 %.

The batch process was started by inoculation with cells from a working cell bank and lasted until the whole glucose was consumed by the bacteria, which was the starting point for the exponential feed. The feed was adjusted in a way that the growth rate μ was 0.1 h^{-1} and was

performed for another three doubling times. After that time a final cell mass of approximately 27 $\frac{\mathrm{gCDM}}{\mathrm{L}}$ was obtained and full induction with 20 $\frac{\mu mol}{gCDM}$ IPTG was performed. After induction the fermentation was run for a time span of about 7 hours. Fermentation was performed either in 20 l or 100 l scale.

2.2.2 Cell harvest

Depending on the fermentation scale two different centrifugation operating procedures were performed for cell harvest

- Contifuge at 17000 rpm with a flow rate of 115 mL/min
- Disk stack centrifuge at 13625 rpm with a flow rate of 100 L/h

2.2.3 Homogenization and cell debris removal

The cell disruption by homogenization was performed at cell densities ranging from 15 to 75 $\frac{\mathrm{gCDM}}{\mathrm{L}}$, either with one passage at 700 bar or with two passages at 70/700 bar.

After homogenization the cell debris were removed by centrifugation, firstly to determine the solid content of the homogenate and finally to get the supernatant in which the GFP was diluted. For the determination of solid content 10 mL of the homogenate were centrifuged in the lab centrifuge for 60 minutes at a speed of 4500 rpm. The debris removal was performed with the Contifuge in 50 mL Greiner tubes for 30 minutes at a speed of 8500 rpm.

2.2.4 Analytics of homogenate supernatant

The turbidity was measured with the turbidimeter after homogenization and the supernatant was measured again after debris removal. For this means at least 10 mL of the liquid were filled into the cuvette.

For the determination of the GFP content fluorescence measurement was performed. The used parameters are shown in Table 3.

Table 3: System settings for infinite M200 Pro measurements.

Parameter	Value
Mode	Fluorescence top reading
Excitation wavelength	485 nm
Excitation bandwidth	9 nm
Emission wavelength	535 nm
Emission bandwidth	20 nm
Sample volume	100 µL
Gain	50 Manual
Numbers of flashes	40
Integration time	20 µs
Lag time	0 µs
Settle time	0 ms
Z-position (Manual)	15437 µm
System	AIAM-ITX-216
Used plate	Nunclon 96 Flat Bottom Black Polystyrol LumiNunc FluoroNunc

2.2.5 Identification of the precipitate

For the identification of the precipitate the first step was to determine whether it is soluble and which solvent can be used. Solubility on the one hand was tested with 0.1, 0.5 and 1.0 M sodium hydroxide and with 0.1 and 1.0 M acetic acid on the other hand. For each approach a final concentration of 1.0 mg/mL was prepared and mixed over night with the rotator at speed step 10. Subsequently, solutions with final concentrations of 10 mg/mL and 100 mg/mL were prepared in 0.1 and 1.0 M sodium hydroxide respectively. These solutions were then diluted and used for SDS-PAGE and protein quantification with the Quant-iT™ Protein Assay Kit. The samples were diluted with the appendant solvent to reach final concentrations between 1.0 mg/mL and 10 mg/mL as preparation for SDS-PAGE. For protein quantification the solutions in 0.1 M NaOH were diluted in a twofold serial dilution, ranging from undiluted to 1:128.

The dry mass of the precipitate was determined by triple determination. Approximately 200 mg were weighed in into glass beakers, dried for 24 hours at 105 °C and cooled down in an ecsicator.

Additionally a buffer exchange via a PD10 column was performed with the 100 mg/mL in 0.1 M NaOH solution. For elution a 10 mM Tris/HCl buffer at pH 7.0 was used. Finally this solution was diluted to a final precipitate concentration of 5 mg/mL and 1 mg/mL and photometer scans from 200 nm to 320 nm were performed respectively.

2.2.6 Precipitation of dissolved impurities

2.2.6.1 Spontaneous precipitation over time

For a first assessment of conditions that lead to the precipitation of the impurities in the clarified homogenate a series of tests was performed. The properties of the used homogenates are shown in Table 4.

Table 4: Used homogenates for spontaneous precipitation experiments.

Cell density [$\frac{gCDM}{L}$]	Homogenization conditions [bar]	Benzonase (9 $\frac{U}{mL}$)
25	0/700	-
25	70/700 1 passage	-
25	70/700 2 passages	-
50	0/700	-
50	70/700 1 passage	-
50	70/700 2 passages	-
50	70/700 2 passages	+
75	0/700	-
75	70/700 1 passage	-
75	70/700 2 passages	-

Those homogenates were filled into 15 mL Greiner tubes and stored at 4 °C and at room temperature for one, four and five days respectively. After the storage time, turbidity was measured and for the clearance of the liquid centrifugation at 4500 rpm for one hour was performed. The solid content was determined volumetric as well as gravimetric. For the gravimetric determination the pellet was resuspended in RO-water, poured into a glass beaker, dried for 24 hours at 105 °C and cooled down in an ecsicator. For analysis of the supernatant fluorescence and turbidity were measured. Additionally SDS-PAGE was performed for the dissolved pellets and the supernatants

2.2.6.2 $CaCl_2$ precipitation

For the precipitation with $CaCl_2$ clarified and heat precipitated homogenates of a 35 $\frac{\mathrm{gCDM}}{\mathrm{L}}$ cell suspension were used respectively. A 0.25 M Na_3PO_4 stock solution was added to the homogenates to reach a final PO_4^{3-} concentration of 0.01 M. The $CaCl_2$ was prepared as 2.0 M stock solution and added in the way to get final concentrations of 25, 50, 100 and 150 mM. The mixtures were shaken well, centrifuged for 15 minutes at 4500 rpm with the lab centrifuge and fluorescence of the supernatant was measured.

Furthermore the pellets of the 25 mM and the 150 mM precipitation were dissolved in 0.1 M NaOH and photometer scans in the range of 220 nm to 320 nm were performed for the dissolutions and the appendant supernatants.

2.2.6.3 Precipitation with PEG

PEG precipitation was performed with a 40 % stock solution of PEG 6000. Firstly, a purified GFP standard was mixed with the PEG stock to reach final contents between 1 and 25 % PEG. After mixing and centrifugation fluorescence was measured. Secondly clarified and unclarified homogenates of 25 and 50 $\frac{\mathrm{gCDM}}{\mathrm{L}}$ were mixed with the stock solution in a way to reach 5, 10, 15, and 20 % PEG. Fluorescence of the supernatant was measured and SDS-PAGE was performed.

2.2.6.4 Heat precipitation

For the first heat precipitation trials cell suspensions with 15, 25 and 50 $\frac{\mathrm{gCDM}}{\mathrm{L}}$ were homogenized with two passages at 70/700 bar. The homogenates were centrifuged, turbidity and fluorescence were measured and they were filled into 15 mL Greiner tubes. Precipitation was performed at 40 °C, 50 °C and 60 °C for one, three, five and 24 hours each. Again turbidity was measured before and after centrifugation, the solid content was determined gravimetric and fluorescence was measured after centrifugation. For the determination of a purification effect SDS-PAGE was performed for the supernatants.

After the first trials, heat precipitation was performed at 50 °C for 3 hours in all the following experiments. Under these conditions clarified and unclarified homogenates with cell suspension concentrations between 20 and 50 $\frac{\mathrm{gCDM}}{\mathrm{L}}$ were used, salt content was varied between 50 and 100 mM NaCl. The analytics have been the same as mentioned above.

Clearance efficiency was determined by filling 13.5 mL of heat treated homogenate into 15 mL Greiner tubes and centrifuging them for 1, 3, 5, 15, 30, 45 and 60 minutes at 4500 rpm with the lab centrifuge. The homogenized cell suspensions had a cell density of 25 and 50 $\frac{\mathrm{gCDM}}{\mathrm{L}}$. For heat precipitation they were used clarified and unclarified. The solid content was measured volumetric and turbidity of the supernatant was measured with the turbidimeter.

2.2.7 Adsorptionisotherms

The isotherms were prepared in 1.5 mL reaction tubes with a reaction volume of 1 mL as shown in Table 5. The volumes were calculated according to equation 2.1 and 2.2. The adsorption isotherms were executed as small scale batch experiments to determine the equilibrium capacity of the used resins.

Table 5: Pipetting scheme for adsorption isotherms.

sample [µL]	slurry [µL]
100	900
300	700
500	500
600	400
700	300
800	200
950	50

$$V_g = \frac{c_0 V - c_i V}{c_0 + x q_i} \quad (2.1)$$

$$V = V_g + V_s \quad (2.2)$$

Where V_g and V are the volume of the gel in the slurry and the overall volume respectively, V_s is defined as the required sample volume, c_0 the concentration of the starting material, c_i the expected supernatant concentration, q_i the expected binding capacity and x is the used concentration. The q_i values were calculated from equation 1.2 for each c_i, where the adsorption constant K_i and the maximum binding capacity q_m were determined according to the pure GFP isotherm.

For the first step the resin, either CaptoQ or Q-Sepharose FF, was washed with buffer for three times and then the slurry concentration was adjusted to 50 %. Then, the resin was pipetted into the 1.5 mL reaction tubes and filled up with sample to 1 mL according to Table 5. Then the tubes were shaken well with the lab shaker and mixed for 24 hours with the rotator at speed step 9. Finally the tubes were centrifuged with the eppendorf centrifuge for 0.5 min at top speed and fluorescence of the supernatant was measured with the Tecan reader.

2.2.8 SDS-PAGE

SDS-PAGE on the one hand was used for determination of the size of proteins in the supernatants and dissolved precipitate, on the other hand for determination of purity and purification effects of the supernatants. The used materials and devices are listed in

Table 1 and Table 2 respectively. The diluted solutions were mixed 3:4 with the sample buffer and heat treated at 75 °C for 15 minutes in the thermoshaker. 15 µL sample and 3 µL MW-standard were pipetted into the wells respectively and the electrophoresis chamber was filled up with 1x running buffer. Electrophoresis was performed with 200 V for 50 minutes. Staining was performed with Coomassie Blue, preheated to 90 °C, for 20 minutes on an orbital shaker, destaining was performed with 10 % (v/v) acetic acid on the orbital shaker.

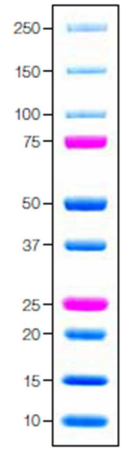

Figure 9: Bands of used Precision Plus Protein standard (Bio Rad)

2.2.9 DNA analytics

Agarose gel electrophoresis was used to show the effects that the purification operations has on the dissolved DNA.

The first step was an RNA digestion with the following approach. After mixing it was incubated for 15 minutes at 37 °C.

Table 6: Used volumes for RNA digestion.

component	volume [µL]
sample	1000
EDTA 1M	120
TRIS-buffer 10 mM	78,8
RNAse 10 U/mL	1,2

The second step was phenol-chloroform extraction. The sample was mixed with the same volume of phenol-chloroform water and mixed until an emulsion was formed. Then it was centrifuged for one minute with the Freso 21 Heraeus centrifuge at 14800 rpm and the aqueous phase was transferred to a fresh tube. This procedure was repeated 2 times. For electrophoresis the sample was mixed 5:6 with the loading dye and 180 µL were loaded to the wells of the agarose gel. Electrophoresis was run for approximately half an hour at 100 V.

For precipitation of the DNA the sample was mixed with 10 vol% 3 M NaAc pH 5 and 2,5 times the volume of 100 % ethanol and stored at -20 °C over night.

3 Results and Discussion

3.1 Identification of the precipitate

In order to get first information about the nature of the precipitate, it was tried to be dissolved in NaOH and CH_3COOH. Additionally, photometer scans were performed with the dissolved precipitate for this means. The solubility tests showed that the precipitate was soluble in each of the applied NaOH concentrations but it was not soluble in CH_3COOH. Figure 10 shows the absorbance spectra of the dissolved precipitates in exchanged buffer at concentrations of 1 mg/mL and 5 mg/mL.

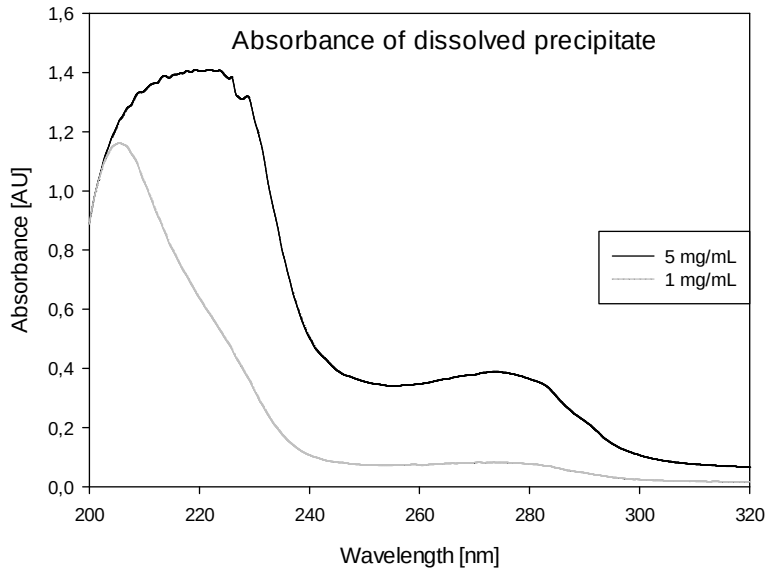

Figure 10: Absorbance of dissolved precipitates from 200 nm to 320 nm. Final concentrations of 1 mg/mL and 5 mg/mL are reached by dilution of 100 mg/mL solution prepared with 0.1 M NaOH.

The absorbance maximum for the 1 mg/mL solution is approximately at 205 nm, which is the characteristic wavelength of peptide bonds. The 260:280 ratio was calculated by dividing the absorbance at 260 nm by the absorbance at 280 nm. The ratios of the two solutions are shown in Table 7.

Table 7: Absorbance of diluted solutions at 260 nm and 280 nm with calculated ratios 260:280.

	Absorbance 260 nm	Absorbance 280 nm	Ratio 260:280
5 mg/mL	0.3484	0.3638	0.9577
1 mg/mL	0.0733	0.0768	0.9544

These ratios suggest, that the precipitates are of high protein content with low portion of nucleic acids, as pure protein solutions have values about 0.57, pure DNA about 1.8 and pure RNA about 2.0. This is caused by the absorbance maximum of aromatic amino acids at 280 nm and the absorbance maximum of nucleic acids at 260 nm. The dry mass determination showed that the mean share of dry solids in the precipitate was 15.65 %. In Figure 11 SDS-PAGE analysis of dissolved spontaneously precipitated pellets is shown. Two different pellet concentrations – 10 (lane 1) and 50 mg/mL (lane 4) - were applied in order to make the differently concentrated proteins visible. Especially the proteins of lower molecular mass below 45 kDa are well visible in lane one, whereas the proteins of higher molecular mass over approximately 50 kDa are better visible in lane 4. Overall, it seems that there is a protein with approximately 250 kDa and then there is a range of proteins with a mass between 150 kDa and 50 kDa visible by a kind of smear over this molecular weight range. Additionally there is a spectrum of bands between 25 and 37 kDa, with a band at the mass of GFP, at approximately 28 kDa. Below 20 kDa again a smear appears with visible bands at approximately 19 and 15 kDa, as well as a band at 10 kDa. Summarizing this analysis there are some proteins in the lower molecular mass range below 20 kDa, a wide range in the middle mass range between 30 and 150 kDa and a protein with approximately 250 kDa.

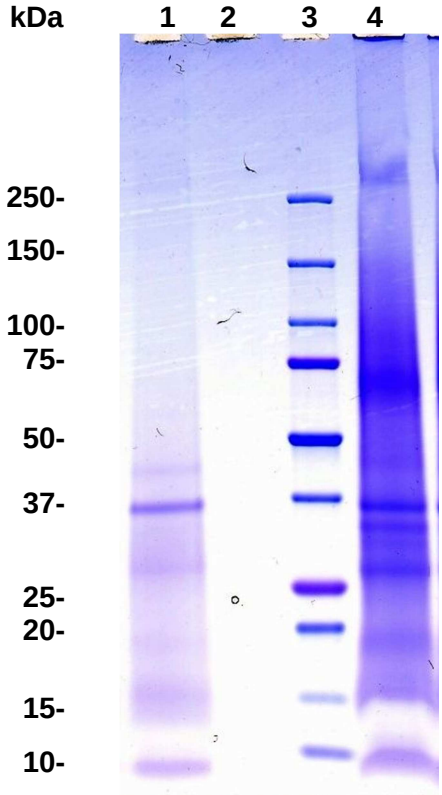

Figure 11: SPS-PAGE gel of dissolved spontaneously precipitated pellet, stained with Coomassie-blue. 1) 10 mg/mL; 2) sample buffer 1:4; 3) MW-Std. 4) 50 mg/mL.

Protein content was calculated by the calibration curve that is shown in Figure 12. The protein content in the 10 mg/mL and 100 mg/mL solution was 1.05 mg/mL and 10.91 mg/mL respectively. Concluding, the dry solids share in the precipitate is composed of approximately two-thirds protein and one-third other components which may be nucleic acids, lipids or other cell wall components.

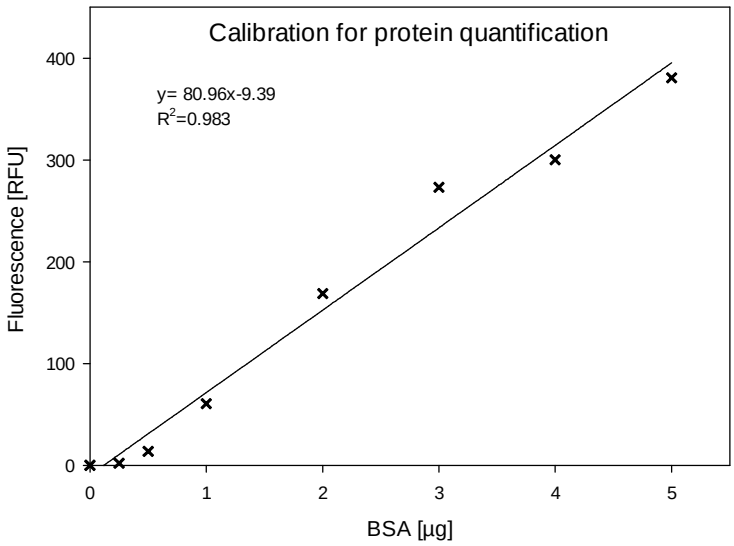

Figure 12: Calibration curve for protein quantification. Fluorescence was measured at 485/590 nm and plotted versus the amount of BSA in µg in the measured sample. Regression was done by linear fit.

Summing up, the precipitate consists of a high amount of water with approximately 15 % dry solids. The dry solids are composed of approximately two thirds of proteins that have a wide range of molecular masses, most of them below 50 kDa.

3.2 Spontaneous precipitation

As a second step, it was necessary to evaluate under which conditions the spontaneous precipitation occurred. In order to get information about these conditions clarified homogenates of 25, 50 and 75 $\frac{\mathrm{gCDM}}{\mathrm{L}}$ and benzonase treated 50 $\frac{\mathrm{gCDM}}{\mathrm{L}}$ were stored at 4 °C and room temperature for 1, 4 and 5 days respectively. The benzonase was used as it was assumed that DNA may play a role in spontaneous precipitation.

Figure 13 shows an overview of the solid contents for the spontaneous precipitation experiments. The solid content was calculated by determining the dry mass of the precipitate, which was centrifuged, resuspended in water and dried. The dry mass was then divided by the volume of used homogenate. In the case of 25 $\frac{\mathrm{gCDM}}{\mathrm{L}}$, especially under cooled conditions, quite few precipitate was formed. At each concentration it was observable, that less precipitate was formed under cooled conditions than at room temperature. The highest amount of precipitate was formed after four days and decreased after day 5. This could be caused by slower formation of agglomerates on the one hand and may represent a kind of solubility equilibrium which is reached slower under cool conditions on the other hand.

At room temperature at least one and a half times the amount of precipitate was formed at each concentration and homogenization condition. Furthermore, the effect that the amount of precipitate decreased between four and five days was not observable. The highest amount of precipitate was formed in the Benzonase treated homogenate. This could be an indication for nucleic acids or fragments of these which stay in solution when they are not further

fractionized, but precipitate by forming agglomerates when they are digested to smaller fragments by Benzonase.

Although the amount of precipitate was a bit higher in the case of standard homogenization at 70/700 bar for two passages, the homogenization conditions did not seem to have a major impact on the precipitation. Whereas the cell density of the homogenized cell suspensions had significant impact on the amount of precipitates.

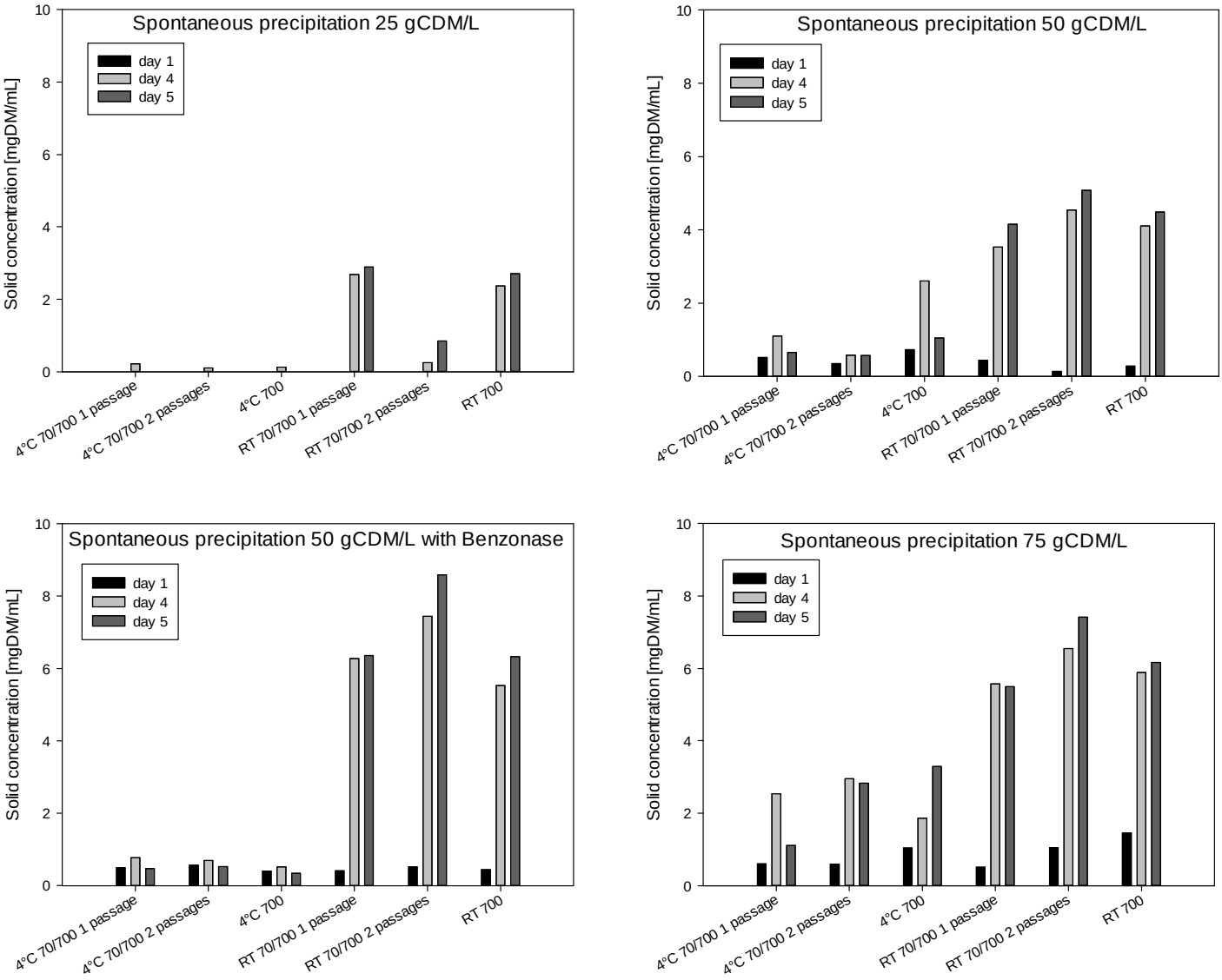

Figure 13: Overview of the gravimetric solid contents for spontaneous precipitation experiments. Experiments were performed with clarified homogenate of 25, 50 and 75 gCDM/L cell suspensions and with benzonase treated clarified homogenate of 50 gCDM/L cell suspension. Abbreviation RT stands for room temperature.

In Figure 14 the relationship between the cell density of the homogenized cell suspension, the amount of formed precipitate after five days and the used homogenization conditions is shown. It is obvious, that especially for 50 $\frac{\mathrm{gCDM}}{\mathrm{L}}$ the homogenization conditions did not have that big impact on the amount of formed precipitate. For the other cell densities only the standard homogenization differs clearly from the others. Overall, it is observable that the amount of precipitate increased linearly with the cell density. This effect is evident, as more disrupted cells are accompanied by more fragments formed by homogenization. The effect that under standard homogenization conditions with 25 $\frac{\mathrm{gCDM}}{\mathrm{L}}$ the amount of precipitate was

less than half the amount of the others could be explained by the fact that simply less cells and compounds were present. The harsher homogenization leads to smaller fragments, which do not interact that well and form agglomerates due to their higher free length of path within the homogenate, as they are dispersed more finely. In contrast to this, the viscosity is decreasing with harsher homogenization conditions, as the DNA gets destroyed more effective. Due to this fact, at higher cell densities more precipitate is formed after homogenization at 70/700 bar for two passages.

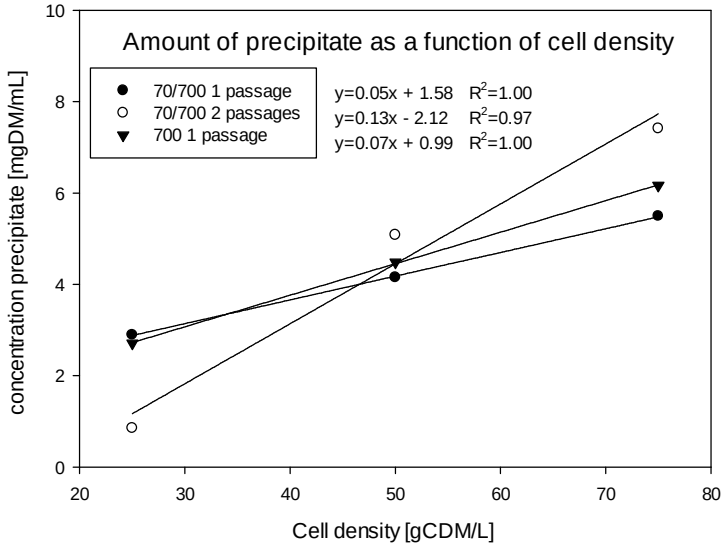

Figure 14: Relationship of homogenized cell suspensions' cell density and amount of spontaneously precipitated solids after five days, for different homogenization conditions. Regression was done by linear fit.

Summing up, it is possible to say that the amount of formed precipitate by spontaneous precipitation over time is dependent on two major conditions, temperature and cell density of the homogenized cell suspension. This correlation between temperature and amount of precipitate lead to the assumption, that precipitation could be influenced actively by the application of heat.

3.3 $CaCl_2$ precipitation

On the basis of the assumption that the displacement effect during IEX could originate from DNA, it was tried to precipitate DNA selectively. As $CaCl_2$ is actually used for precipitation of DNA it was determined if it is capable as a purification step for GFP. It was used as precipitating agent in clarified and heat precipitated homogenates of 35 $\frac{\mathrm{gCDM}}{\mathrm{L}}$ cell suspension respectively. GFP content is shown as a function of $CaCl_2$ concentration in Figure 15.

As Figure 15 shows, even at low $CaCl_2$ concentrations the loss of GFP was quite high. GFP content was approximately halved at 25 mM $CaCl_2$ in the heat precipitated homogenate and at 50 mM in the clarified homogenate.

Based on these results it was decided, that $CaCl_2$ is not capable for the purification of GFP within this process.

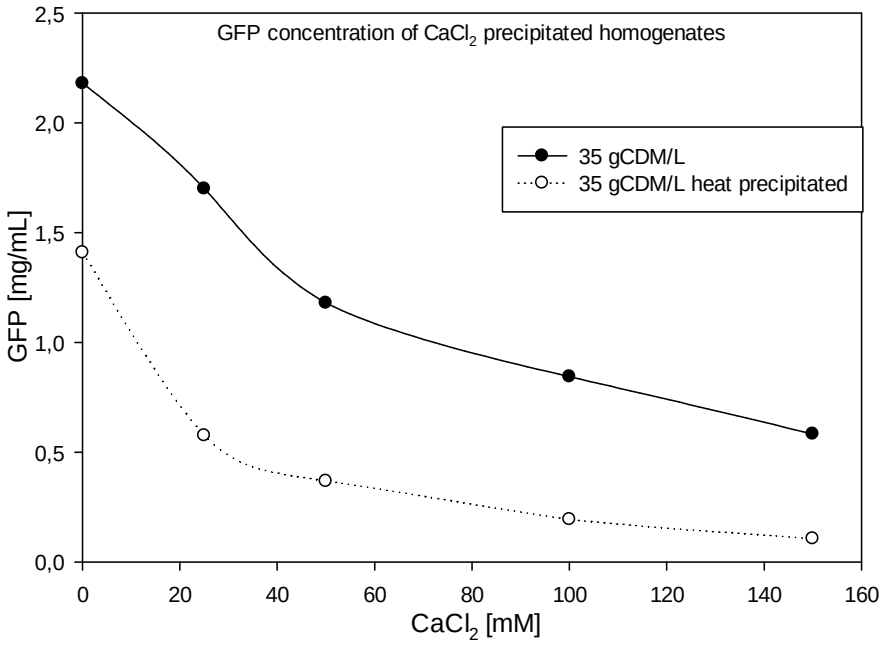

Figure 15: Evolution of GFP content [mg/mL] as a function of $CaCl_2$ concentration [mM].The used homogenates were homogenized at a cell density of 35 gCDM/L at 70/700 bar for 2 passages.

3.4 PEG precipitation

Another approach was to precipitate the impurities with PEG. Firstly, it was determined if purified GFP in solution is precipitated by PEG. As shown in Figure 16 the GFP content did not decrease in the GFP standard with the used PEG concentrations.

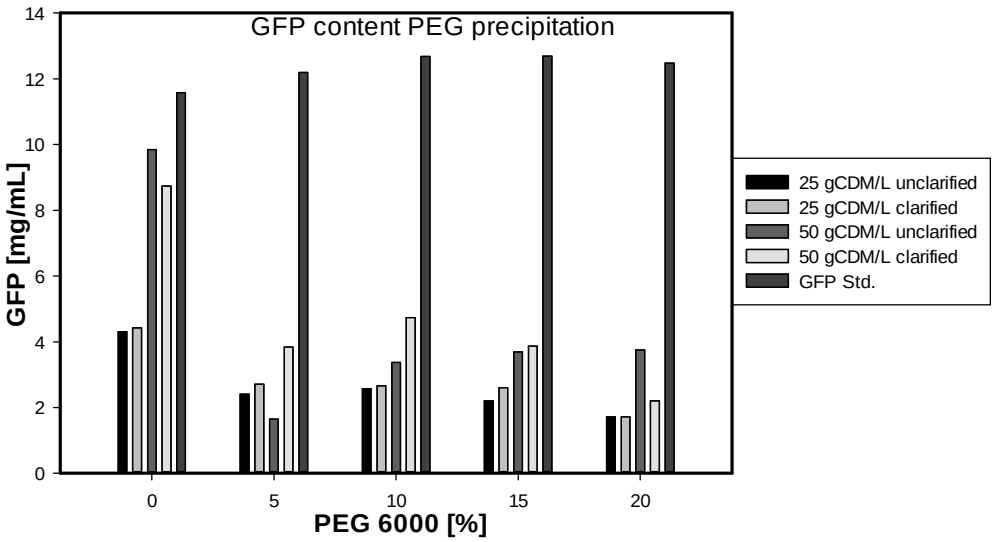

Figure 16: GFP content [mg/mL] at different PEG 6000 concentrations [%]. Used homogenates were 25 and 50 gCDM/L clarified and unclarified respectively. Additionally a purified GFP standard was used.

The slight increase of GFP content with increasing PEG concentration in the GFP standard maybe was caused by a change of the refractive index of the solution, caused by the high viscous and dense PEG. As GFP did not precipitate from the standard solution over the used PEG concentration range, it was decided to perform trials with clarified and unclarified homogenates of 25 and 50 $\frac{\mathrm{gCDM}}{\mathrm{L}}$ cell suspensions. In contrast to results with pure protein, GFP content decreased significantly after addition of PEG. It seems that proteins contained in crude homogenate interact with GFP which evidently leads to a kind of coprecipitation.

Some of the interacting proteins seemed to be reduced by centrifugation as at almost all PEG concentrations the GFP reduction was less in clarified homogenates than in the unclarified ones. Results of SDS-PAGE analysis of the supernatants are shown in Figure 17.

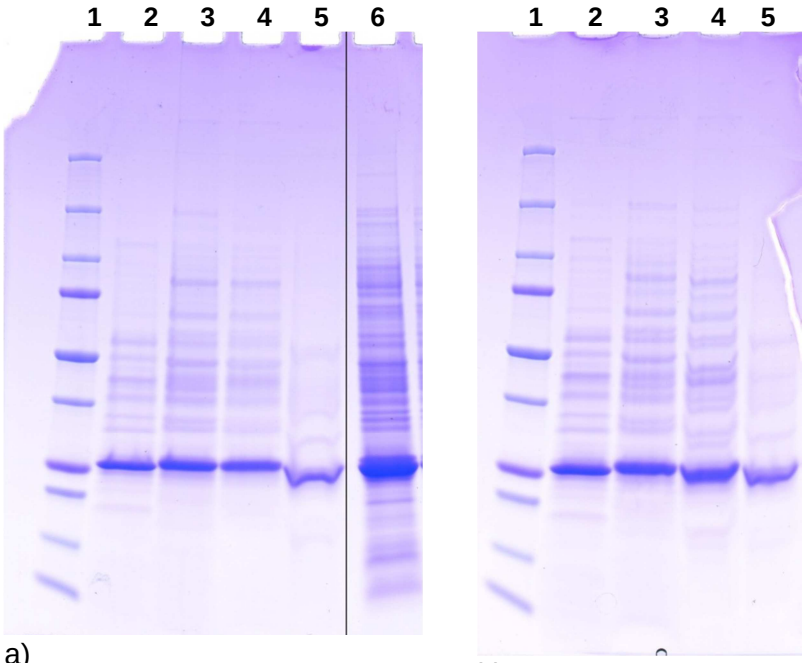

Figure 17: SDS-PAGE gels of PEG precipitation supernatants. a) 25 gCDM/L unclarified 1) MW Std. 2) 5 % PEG; 3) 10 % PEG; 4) 15 % PEG; 5) 20 % PEG; 6) homogenate; b) 25 gCDM/L clarified 1) MW Std. 2) 5 % PEG; 3) 10 % PEG; 4) 15 % PEG; 5) 20 % PEG.

SDS-PAGE showed that the purification effect by PEG was quite high. Especially proteins of lower molecular weight were removed already at low PEG concentrations and the smear at higher molecular masses is reduced evidently. Nonetheless, GFP also was removed which is observable by the reduction of the characteristic band in comparison to the crude homogenate.

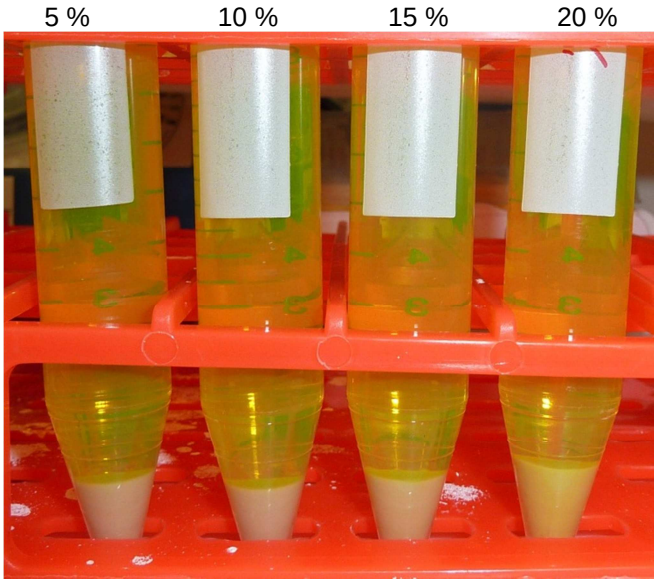

Figure 18: PEG precipitation of unclarified 25 gCDM/L homogenate with 5, 10, 15 and 20 % PEG

Figure 18 shows the precipitation of unclarified 25 $\frac{\mathrm{gCDM}}{\mathrm{L}}$ homogenate with increasing concentration of PEG. It is visible that at 20 % PEG the precipitate was already coloured green which indicates coprecipitation of GFP.

Due to these results PEG precipitation was not considered as a purification step for GFP directly after homogenization as the loss of GFP is too high.

3.5 Heat precipitation

3.5.1 Assessment of heat precipitation conditions.

Heat precipitation was supposed being a capable purification step, as the spontaneous precipitation was more effective at room temperature and GFP is quite stable to heat as literature showed. For the evaluation of heat precipitation, homogenates of 15, 25 and 50 $\frac{\mathrm{gCDM}}{\mathrm{L}}$ were incubated at 40, 50 and 60 °C for a duration between 1 and 24 hours respectively. After heat treatment the precipitates were separated by centrifugation and supernatants and pellets were analysed.

An overview of the solid contents after heat precipitation over time is given in percent weight per weight in Figure 19. For almost all concentration - temperature combinations that were used to precipitate the impurities by heat, it is observable that the amount of precipitate increased with time. Secondly, within the homogenates that were incubated at one temperature the amount of precipitate was increasing with the homogenates' cell densities and finally it was observable that higher temperature results in a higher amount of precipitate. The amount ranges from the lowest effect with 0.23 % (w/w) in the 15 $\frac{\mathrm{gCDM}}{\mathrm{L}}$ homogenate after 1 hour at 40 °C, up to the highest effect with 14.42 % (w/w) in the 50 $\frac{\mathrm{gCDM}}{\mathrm{L}}$ homogenate after 24 hours at 60 °C. Figure 20 shows the development of the GFP content, in mg/mL, in the clarified homogenate before and after heat precipitation over time. The amount of functional GFP was decreasing over time at each temperature. After three hours, the loss of functional GFP was approximately 20 % at 40 °C and 50°C for each homogenate and even after 24 hours the maximum loss was only 30 % at these temperatures. Thus GFP seems to be quite stable under these conditions. At 60 °C there was a massive loss of functional GFP over time. After 1 hour the loss amounted about 30 % and after 3 hours it was already over 40 % for each homogenate. Finally almost the entire fluorescence was lost after 24 hours.

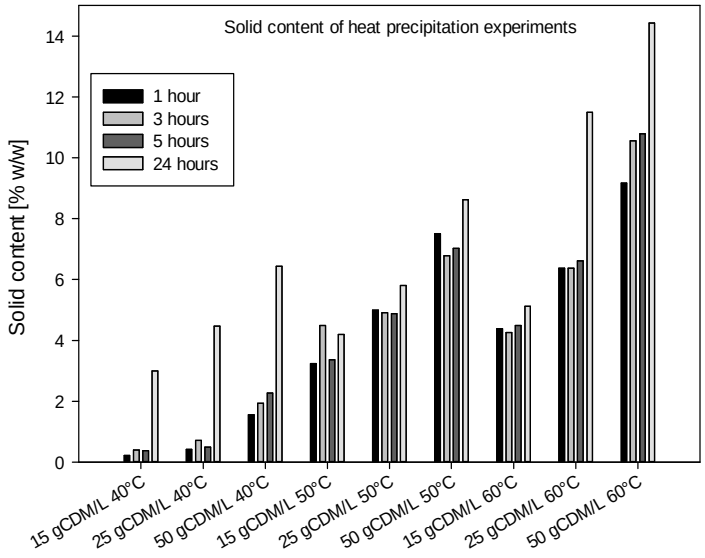

Figure 19: Solid contents in heat precipitated homogenates. 15, 25 and 50 gCDM/L cell suspensions, were homogenized at 70/700 bar for 2 passages and clarified by centrifugation. Then they were incubated at 40, 50 and 60 °C for 1, 3, 5 and 24 hours and centrifuged with the lab centrifuge for 60 minutes at 4500 rpm.

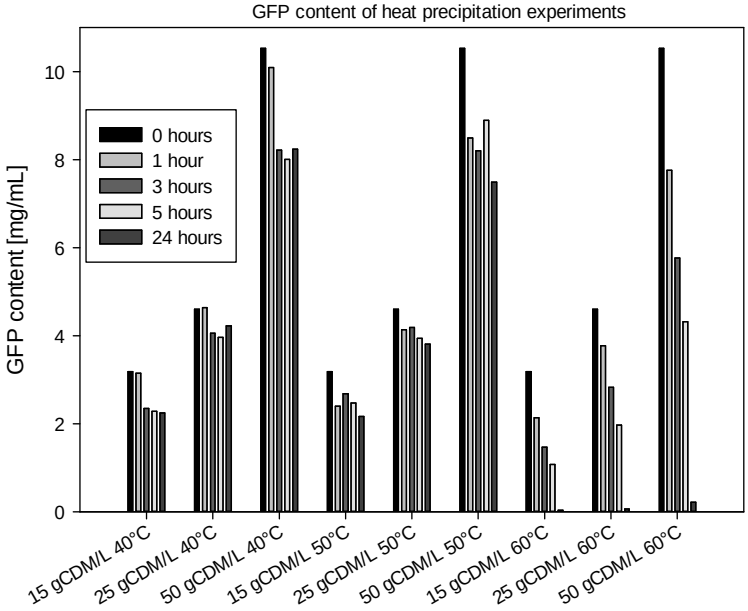

Figure 20: GFP content of clarified heat precipitated homogenates. The concentration was measured before precipitation and after 1, 3, 5 and 24 hours of heat precipitation. Heat precipitation was performed with clarified homogenates of 15, 25 and 50 gCDM/L cell suspensions. Afterwards the suspensions were centrifuged with the lab centrifuge at 4500 rpm for 60 minutes.

It seems that GFP either gets denatured at 60 °C in the homogenate or it is co-precipitated by the high amount of precipitated solids. At 60 °C the decrease of the GFP content could be described by an exponential function, as shown in Figure 21. When the GFP content was made dimensionless by dividing c_t, the concentration after a time interval, by the initial concentration c_0 an exponential relation between content and time was describable independent of the homogenized cell density. The relation is shown in equation 3.1 where *t* is the incubation time, *0.93* is the maximum value for c/c_0 and *-0.188* is the GFP concentration reduction factor.

$$\frac{c_t}{c_0} = 0.93 \cdot e^{-0.188t} \qquad 3.1$$

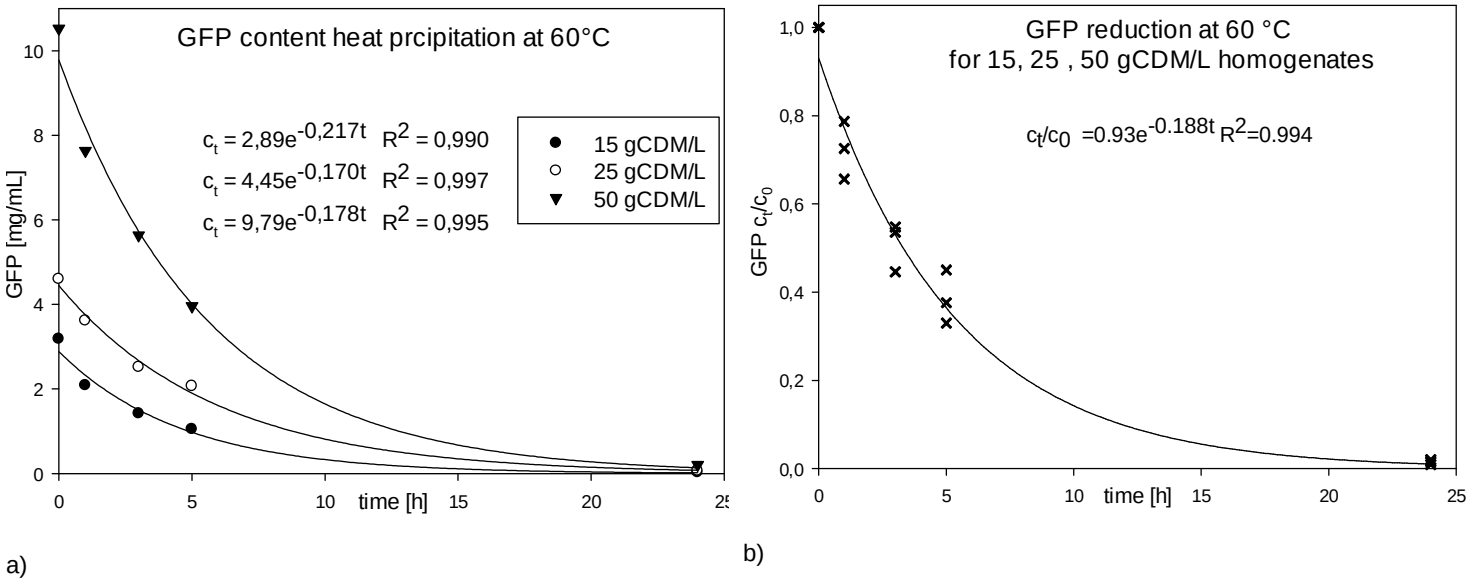

a) b)

Figure 21: GFP content over time at 60°C a) GFP content in 15, 25 and 50 gCDM/L homogenates after heat precipitation over time. Regression was done by exponential fit. b) Dimensionless GFP content over time.

The values for turbidity and clearance efficiency of the tests mentioned above are shown in Table 8 and were interpreted as follows. Turbidity was plotted as a function of time in Figure 22, where it is observable that there was an almost linear increase of turbidity at 40 °C and logarithmic increase at 50 and 60 °C.

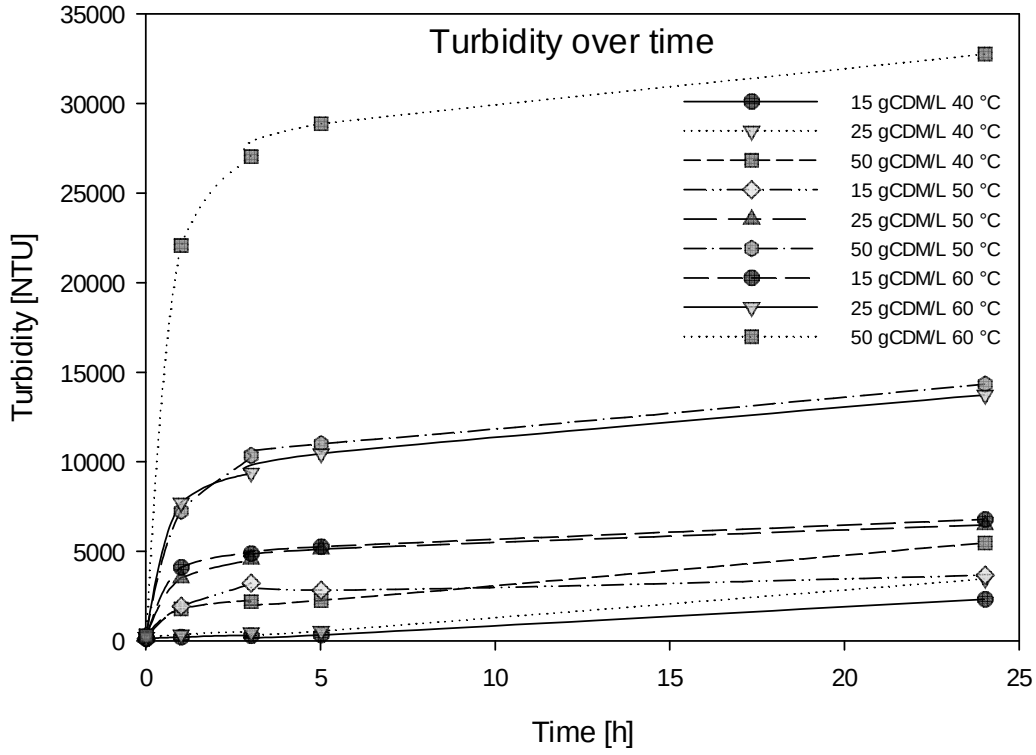

Figure 22: Turbidity of heat precipitated homogenates over time for 15, 25 and 50 gCDM/L at 40, 50 and 60 °C respectively.

Table 8: Turbidity and clearance efficiency of heat precipitated homogenates. Centrifugation was performed with the lab centrifuge at 4500 rpm for 1 hour.

		15 gCDM/L			25 gCDM/L			50 gCDM/L		
Temperature [°C]	**time [hours]**	**turbidity feed [NTU]**	**turbidity effluent [NTU]**	**clearance efficiency [%]**	**turbidity feed [NTU]**	**turbidity effluent [NTU]**	**clearance efficiency [%]**	**turbidity feed [NTU]**	**turbidity effluent [NTU]**	**clearance efficiency [%]**
40	**0**	-	130.0	-	-	214.0	-	-	289.0	-
	1	210.5	192.5	8.6	353.0	318.5	9.8	1795	557.5	68.9
	3	288.0	255.0	11.5	482.0	421.5	12.6	2200	719.5	67.3
	5	331.5	285.5	13.9	550.0	475.5	13.5	2260	846.5	62.5
	24	2330	41.7	98.2	3460	59.5	98.3	5470	150.5	97.2
50	**0**	-	130.0	-	-	214.0	-	-	289.0	-
	1	1939	361.5	81.4	3510	186.0	94.7	7250	106.5	98.5
	3	3230	69.9	97.8	4580	89.9	98.0	10350	101.0	99.0
	5	2832	80.9	97.1	5120	92.2	98.2	11000	103.0	99.1
	24	3669	45.9	98.7	6480	83.5	98.7	14340	94.8	99.3
60	**0**	-	130.0	-	-	214.0	-	-	289.0	-
	1	4100	38.6	99.1	7710	78.3	99.0	22080	99.9	99.5
	3	4875	35.0	99.3	9375	73.9	99.2	27045	97.1	99.6
	5	5260	32.8	99.4	10460	71.5	99.3	28880	87.8	99.7
	24	6780	27.7	99.6	13740	60.0	99.6	32760	74.1	99.8

Taking a look at the turbidity of the heat precipitated homogenates before centrifugation it is observable, that it was influenced by precipitation temperature, duration and the homogenized cell suspensions' cell densities. The turbidity increased with each of these three factors.

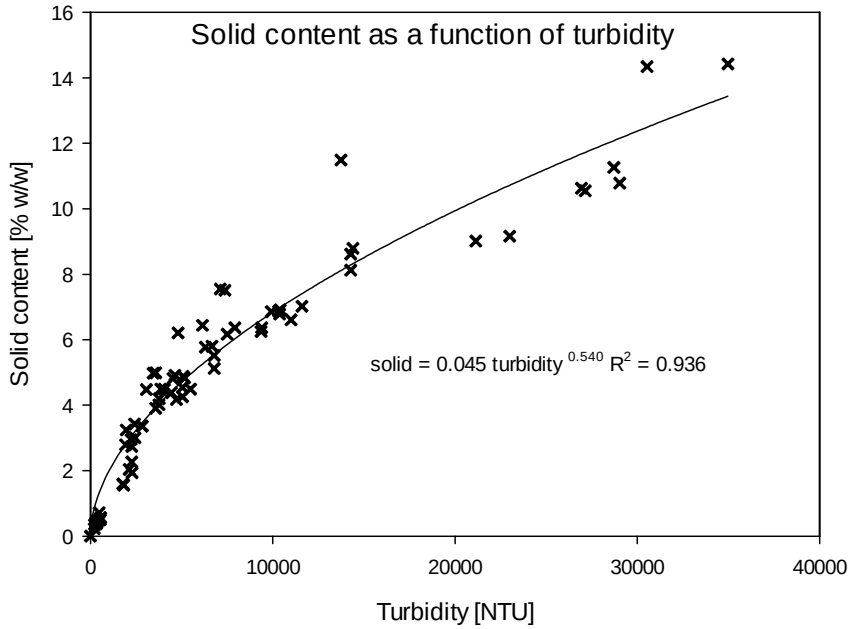

Figure 23: Wet solid content [% w/w] as a function of turbidity [NTU].

Figure 23 shows the relationship between the turbidity and separable solid content. The gravimetric wet solid content is shown as a function of turbidity. The values were determined as duplicates at each temperature and duration. For regression a power equation was used with the result shown in equation 3.2.

$$solid = 0.045 \cdot turbidity^{0.54} \qquad 3.2$$

This equation shows a nonlinear relationship between the solid content and the turbidity and can be used to estimate the actual solid content, in % w/w, depending on the measured turbidity. When this equation is further adapted to equation 3.3 it is possible to calculate the dry solid content ω, where *0.15* is the dry solid factor.

$$\omega = 0.045 \cdot turbidity^{0.54} \cdot 0.15 \qquad 3.3$$

For further analysis the dry solids were calculated by this equation, using the values of turbidity from Table 8. The resulted values for the amount of dry solids were then plotted against time and fitted by kinetic equations of 1st and 2nd order. The differential rate equation for precipitation and its analytical solution for 1st order are shown in equation 3.4 and 3.5, those for 2nd order in equation 3.6 and 3.7 respectively. ω is the dry solid content, ω_{max} is the maximum dry solid content, k is the rate constant and t the time in hours. The units for k are s^{-1} for 1st order and $\% \frac{w}{w} \cdot s^{-1}$ for 2nd order. The values for the rate constant in dependence on temperature and reaction order are shown in Table 9, where R^2 is the coefficient of determination for the different fits

$$\frac{d\omega}{dt} = -k\omega \qquad 3.4$$

$$\omega = \omega_{max} \cdot (1 - e^{-kt}) \qquad 3.5$$

$$\frac{d\omega}{dt} = -k\omega^2 \quad 3.6$$

$$\omega = \omega_{max} \cdot \left(1 - \frac{1}{1 + \omega_{max} kt}\right) \quad 3.7$$

Table 9: Kinetic data for formation of precipitate.

T [K]	Cell density $[\frac{\mathbf{gCDM}}{\mathbf{L}}]$	Order	R^2	ω_{max} $[\%\frac{w}{w}]$	k $[s^{-1}]/[\%\frac{w}{w} \cdot s^{-1}]$	ln (k)
313.15	15	1	0.937	0.476	0,10	-2,263
	15	2	0.943	0.643	0,14	-2,002
	25	1	0.921	0.584	0,11	-2,189
	25	2	0.929	0.771	0,13	-2,064
	50	1	0.825	0.544	1,01	0,010
	50	2	0.908	0.652	1,39	0,329
323.15	15	1	0.985	0.533	1,39	0,329
	15	2	0.989	0.569	4,28	1,454
	25	1	0.979	0.702	1,47	0,385
	25	2	0.995	0.756	3,17	1,154
	50	1	0.977	1.08	1,37	0,315
	50	2	0.995	1.17	1,82	0,599
333.15	15	1	0.977	0.716	1,78	0,577
	15	2	0.991	0.762	4,20	1,435
	25	1	0.970	1.04	1,65	0,501
	25	2	0.989	1.12	2,42	0,884
	50	1	0.993	1.75	1,91	0,647
	50	2	0.999	1.83	2,31	0,837

The Arrhenius equation is shown in equation 3.8, where *A* is the frequency factor, E_a is the activation energy, *R* is the ideal gas constant (8.31 J/molK) and *T* is the temperature in Kelvin.

$$k = A \cdot e^{-E_a/RT} \quad 3.8$$

In order to calculate A and E_a ln(k) was plotted as a function of the reciprocal temperature as shown in Figure 24 and Figure 25. Calculation of E_a and A was only performed in the range between 50 and 60 °C as it seemed, that at 40 °C the process of precipitation was going on too slow. Thus the state of equilibrium is not reached during incubation time and the resulting k values do not fit to the kinetic models.

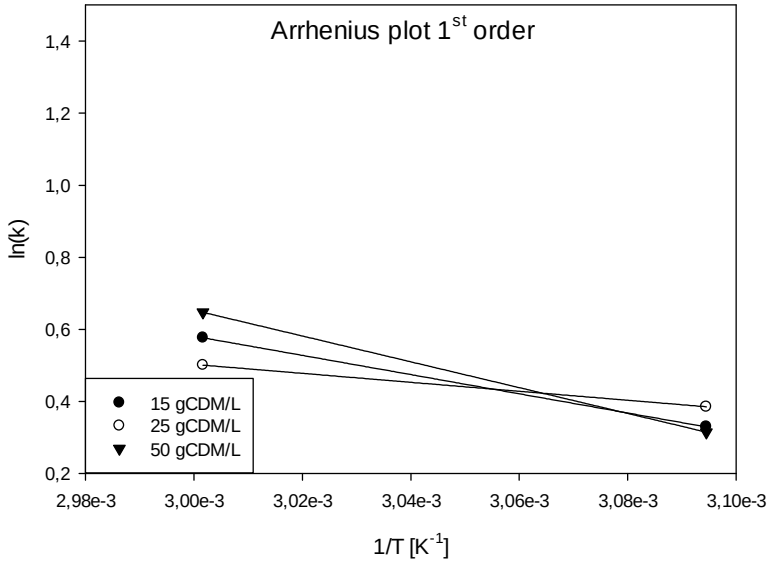

Figure 24: Arrhenius plot for 1st order reaction.

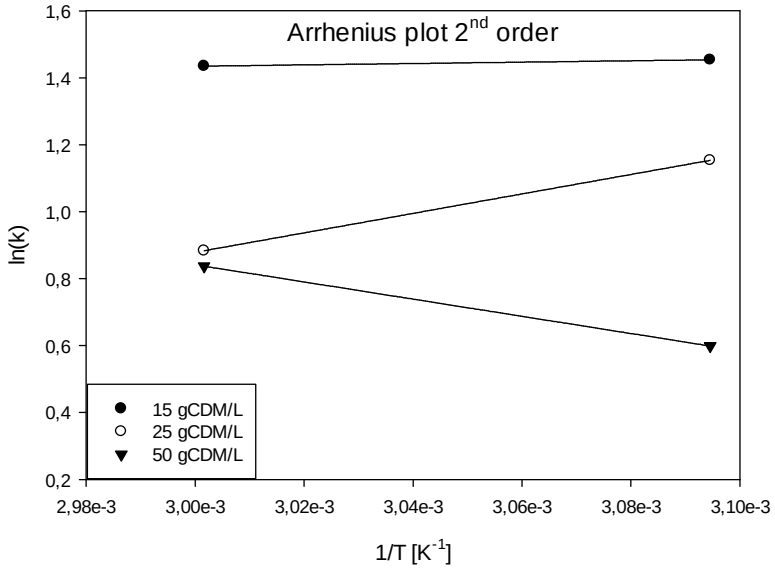

Figure 25: Arrhenius plot for 2nd order reaction.

According to these plots A and E_a can be calculated as it applies that:

$$intercept = \ln(A) \tag{3.9}$$

$$slope = \frac{-E_a}{R} \tag{3.10}$$

Table 10: Results for A and E_a depending on reaction order and cell density.

Order	Cell density $[\frac{\mathbf{gCDM}}{\mathbf{L}}]$	A [s^{-1}]	E_a [$\frac{kJ}{mol}$]	Average	Stddev.
1	15	5.26E+03	22.13	20.73	9.77
	25	6.90E+01	10.33		
	50	8.80E+04	29.73		
2	15	1.78E+10	-1.69	-1.50	22.74
	25	1.45E+02	-24.15		
	50	1.78E+10	21.33		

The values for the rate constants at different temperatures show that the formation of precipitate is strongly dependent on temperature. Taking a look at the Arrhenius plots and the corresponding values for E_a, it seems that a reaction of 1st order is more likely for the precipitation of the proteins than a 2nd order reaction. This can be assumed, as the slopes of the regression lines are lying more closely together for 1st order, whereas the lines for 2nd order are strongly antiparallel. Due to this fact the 1st order values for E_a are not that widespread and thus the standard deviation is distinctive lower. Additionally for 2nd order negative values for E_a are resulting which is not usual. According to these results an average value for E_a of 20.73 kJ/mol could be calculated for the precipitation of the dissolved proteins. This value for E_a seems quite low as for example human serum albumin has an E_a of approximately 100.5 kJ/mol (Bischof 2005). Although the molecular mass of serum albumin, approximately 66 kDa, is in the range of the average molecular mass of the precipitate, it has about five times the activation energy. This could be caused, as the precipitated protein stems from bacterial cells and so has less post translational modifications, which makes the proteins less robust. Another reason for the lower E_a could be that the proteins are already damaged to a certain degree because of homogenization and so less energy is needed to denature them. Considering these points the value for E_a seems to be quite plausible.

Summing up, the rate constant is highly dependent on the temperature. At 40 °C, the rate constant is approximately only one-tenth of the value at 50 °C and thus it seems that at this temperature the precipitation does not go on thoroughly. But at higher temperatures it is possible to suggest a kinetic of 1st order for precipitation.

The clearance efficiency, which was calculated by equation 3.11 was increasing with turbidity.

$$clearance\ efficiency = 1 - \frac{NTU_{effluent}}{NTU_{feed}} \cdot 100 \qquad 3.11$$

Although the turbidity was rising at 40 °C and thus agglomeration is going on, especially for low cell densities the clearance efficiency was very low except for 24 hours incubation time. This also corresponds to the low amount of centrifuged solids in these suspensions. At 50 °C the turbidity has increased at least tenfold already after 1 hour of heat treatment. Clearance efficiency after 1 hour was only below 90 % for 15 $\frac{\mathrm{gCDM}}{\mathrm{L}}$, but rose to approximately 98 % after 3 hours for each homogenate. The highest increase of turbidity was observable at 60 °C, where it was nearly 80 times the initial value after 1 hour treating the 50 $\frac{\mathrm{gCDM}}{\mathrm{L}}$ homogenate. Thus it was even higher than the turbidity of 25 $\frac{\mathrm{gCDM}}{\mathrm{L}}$ homogenate after 24 hours of heat treatment. For each homogenate the clearance efficiency is at least 90 % after one hour at 60 °C. Figure 26 shows the clearance efficiency as a function of turbidity and time, as well as the turbidity as a function of time and temperature for 15, 25 and 50 $\frac{\mathrm{gCDM}}{\mathrm{L}}$ respectively. The used values are the means of duplicate determinations. These diagrams show that the clearance efficiency is increasing with turbidity on the one hand and that the magnitude of the increase of turbidity depends on the temperature, incubation time and cell density of the homogenized cell suspension on the other hand. Thus the higher turbidity which is caused by higher solid content results in higher clearance efficiency.

Comparing the turbidity of the homogenates before and after heat treatment, a reduction was observable only after 24 hours at 40 °C. At 50 °C it was already observable after 1 hour for 25 and 50 $\frac{\mathrm{gCDM}}{\mathrm{L}}$, after 3 hours it was observable for each used cell density, which was true after 1 hour at 60 °C .

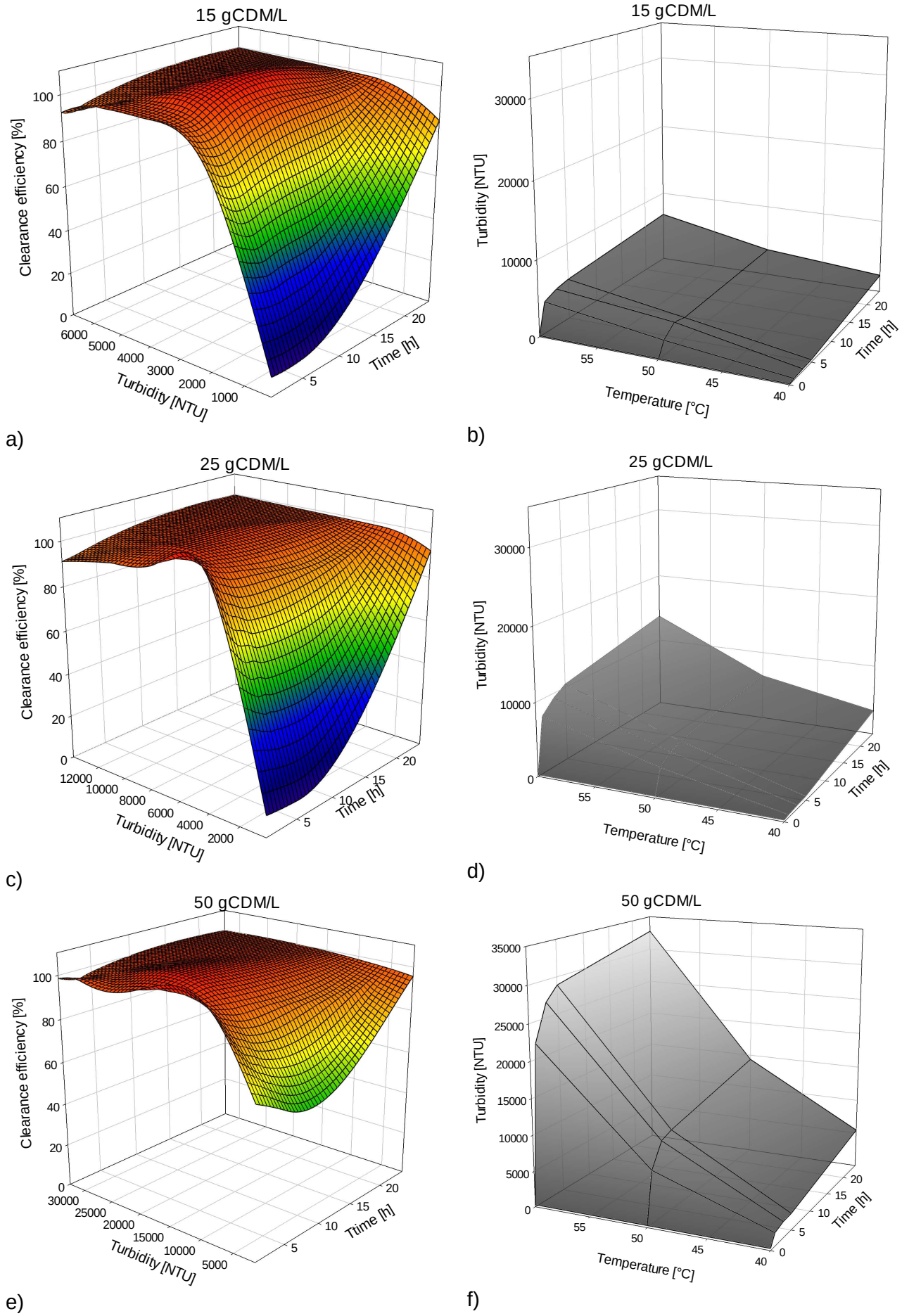

Figure 26: a, c and d clearance efficiency as a function of turbidity and time, b, d and e turbidity as a function of temperature and time for 15, 25 and 50 gCDM/L respectively.

In summary, heat treatment leads to a change of the impurities' properties. The impurities, which are mainly a range of host cell proteins agglomerate faster than they do spontaneously, which is indicated by a rise in turbidity and solid content. This effect is depending on concentration, temperature and duration of heat treatment. By forming agglomerates the particle diameter D_p, and the particle density ρ_p are increasing which leads to a higher settling velocity u_g according to Stoke's law:

$$u_g = \frac{\rho_p - \rho_L}{18\mu} \cdot D_p^2 g \qquad 3.12$$

Where ρ_L is the density of the liquid, μ is the viscosity of the liquid and g is gravitational acceleration. Thus the bigger and denser the particles get by agglomeration, the faster they settle down, which leads to higher clearance efficiencies. The effect, that turbidity was rising during heat treatment but low clearance efficiencies were achieved, which is observable at low cell densities, low temperature and relatively short duration, may be explained by formation of smaller agglomerates. Under these conditions on the one hand the concentration of impurities is lower so fewer proteins can interact to form agglomerates and on the other hand agglomeration is slower due to the lower temperature. The smaller agglomerates do not settle down that fast and are not separated by centrifugation. Higher concentration and temperature lead to faster agglomeration and higher clearance efficiency.

Additionally trials with homogenates of 35 $\frac{\mathrm{gCDM}}{\mathrm{L}}$ cell suspension were performed in order to compare solid and GFP contents as a function of number of passages and heat precipitation. The results of these trials are shown in Figure 27. For heat precipitation the unclarified homogenate after two passages was used. It was observable that the solid content was decreasing from cell suspension to the first passage of homogenization and further decreasing to the second passage. After heat precipitation the solid content increased evidently. This effect shows that on the one hand compaction increases with rising number of passages and on the other hand small particles that are not separable by centrifugation are formed by homogenization. These small particles are agglomerated by heat and get separable by this operational step, thus solid content is rising.

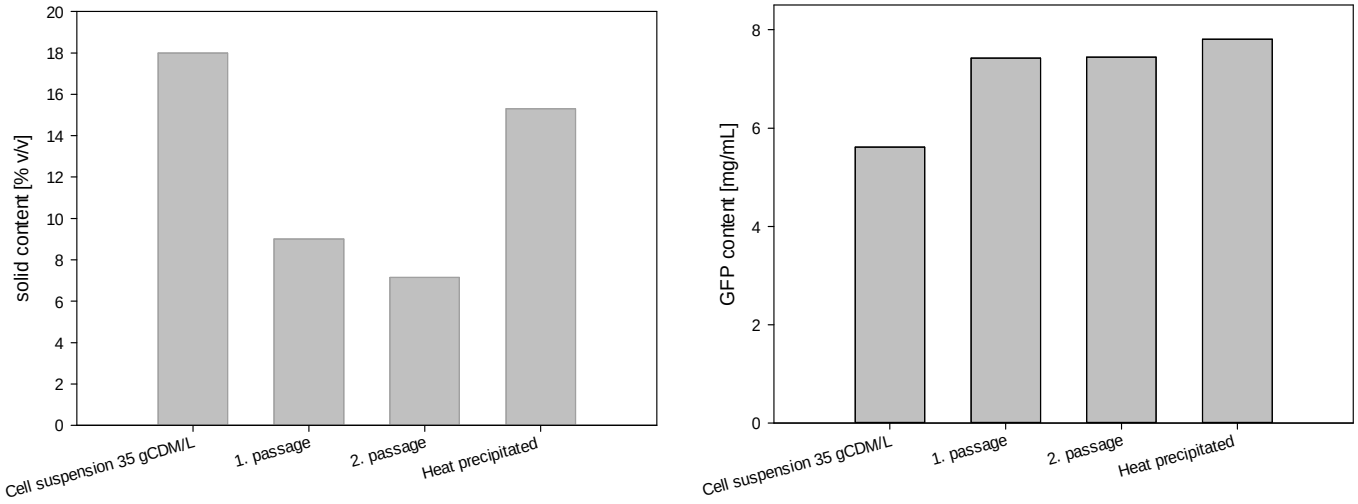

Figure 27: Volumetric solid [%v/v] and GFP contents [mg/mL] of 35 gCDM/L cell suspension and appendant homogenates after 1 and 2 passages at 70/700 bar and 2 passages homogenates' after heat precipitation. Salinity in homogenization buffer was 50 mM NaCl.

GFP content was rising after homogenization this was caused by the breakage of the cells which released the GFP. After heat precipitation it rose again, which may be caused by the

lower turbidity of the supernatant and a higher resulting signal as less particles influence the measurement. However clearance efficiency only reached 91 % and final turbidity of the heat precipitated homogenate was 1320 NTU which is comparably high. Summarizing, it seems that lower salinity results in less efficient heat precipitation.

According to the results mentioned above, the chosen conditions for heat precipitation are 3 hours at 50 °C, since high clearance efficiency, relatively low loss of GFP and a reduction of the initial turbidity of the homogenates are reached.

3.5.2 Centrifugation performance

Centrifugation performance was tested with homogenates that have either been clarified or not after homogenization, to evaluate if it is necessary to remove debris beforehand or if it is possible to save one centrifugation step. The results for solid contents and clearance efficiencies over time are shown in Figure 28. The volumetric solid content showed an increase for the first two measurements after 1 and 5 minutes but a decrease from the measurement after 15 minutes onwards. This effect was caused by compaction. But if the solid content is observed in conjunction with the clearance efficiency, which was calculated by equation 3.11, it is visible that even after this period separation of solids took place as the turbidity was decreasing. Until 30 minutes clearance efficiency was rising evidently, after this period it rose only slightly. After 30 minutes almost all separable solids were centrifuged, which was indicated by relatively stable turbidity. From this period onwards the pellet was compacted by the centrifugation. The turbidity and clarification values for centrifugation performance tests are shown in Table 11.

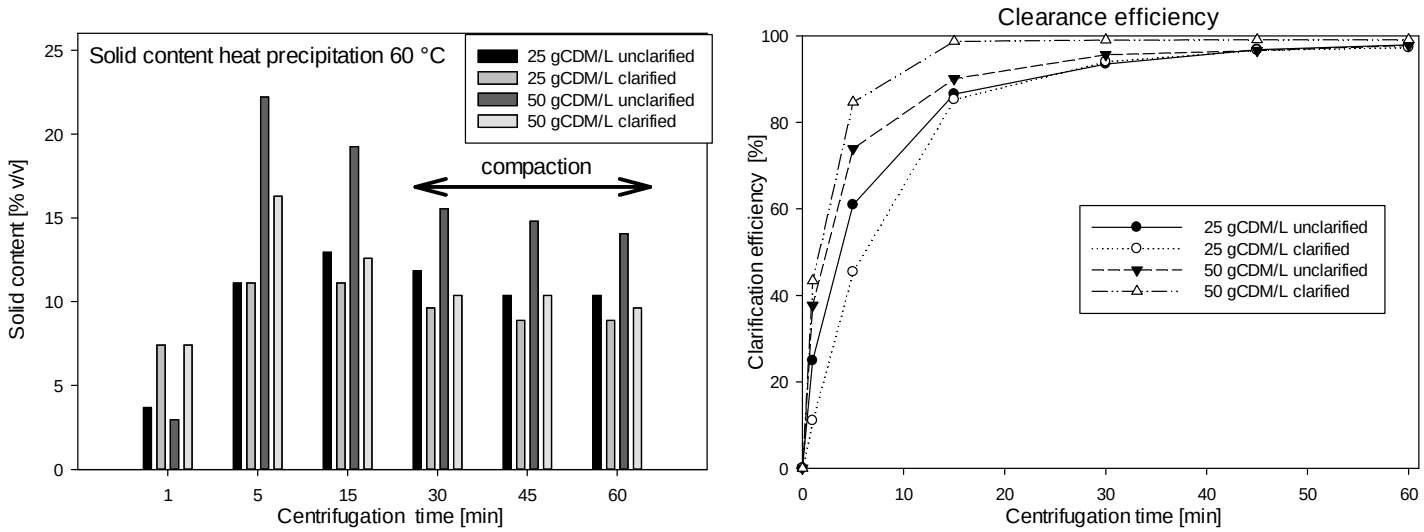

a) b)

Figure 28: Clarified and unclarified heat precipitated homogenates. Centrifuged with the lab centrifuge at 4500 rpm. Cell suspensions had cell densities of 25 and 50 gCDM/L. a) Volumetric solid contents over time. b) Clearance efficiency over time.

Table 11: Turbidity and clearance efficiency of centrifugation performance tests. Duration was as it is given in the table, centrifugation was performed with the lab centrifuge at 4500 rpm.

	25 gCDM/L clarified			25 gCDM/L unclarified		
time [min]	**turbidity feed [NTU]**	**turbidity effluent [NTU]**	**clearance efficiency [%]**	**turbidity feed [NTU]**	**turbidity effluent [NTU]**	**clearance efficiency [%]**
1	5430	4800	11.6	14850	11190	24.6
5	5370	2943	45.2	14400	5820	59.6
15	5400	794	85.3	15000	2007	86.6
30	5460	322	94.1	14970	966.4	93.5
45	5370	180	96.6	14880	472	96.8
60	5340	145	97.3	15300	313	98.0
	50 gCDM/L clarified			**50 gCDM/L unclarified**		
1	10170	5730	43.7	27180	16350	39.8
5	10170	1551	84.7	26280	6840	74.0
15	9900	129	98.7	26880	2601	90.3
30	9930	97.2	99.0	24720	1147	95.4
45	10260	91.9	99.1	26160	890	96.6
60	10290	90.2	99.1	26220	578	97.8

Here the clearance efficiency was the highest for the clarified 50 $\frac{\text{gCDM}}{\text{L}}$ homogenate where also lowest turbidity was reached after heat treatment. Indeed clearance efficiency was at least 97 % for each homogenate. The approach with clarified 50 $\frac{\text{gCDM}}{\text{L}}$ is shown in Figure 29. After these trials, it was decided to use unclarified homogenates as one centrifugation step is saved by this operational procedure.

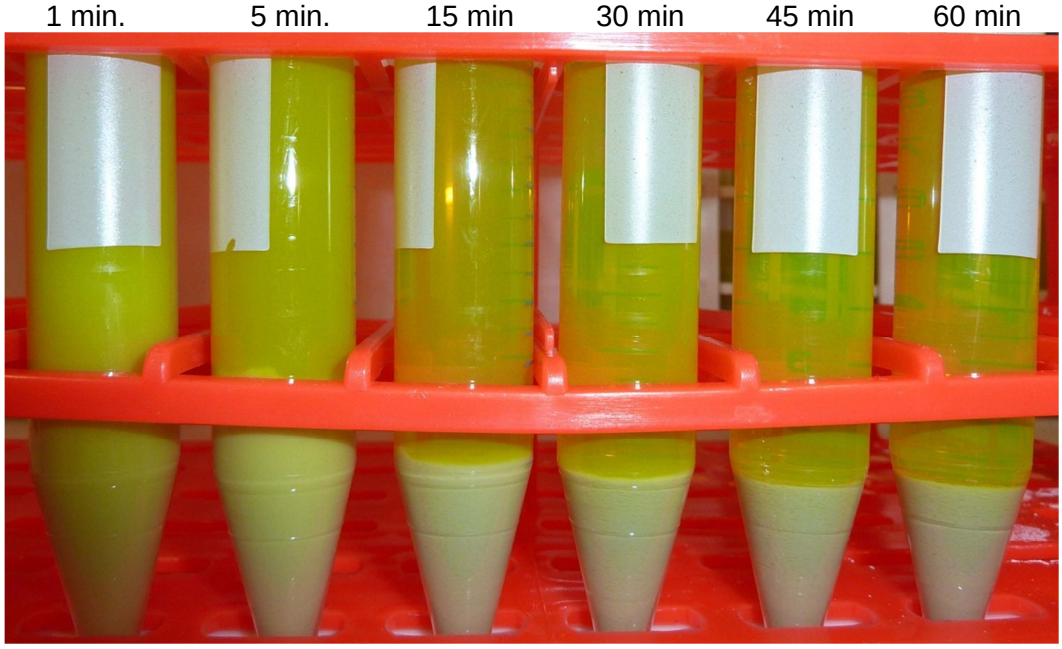

Figure 29: Progress over time of centrifugation of clarified 50 gCDM/L homogenate after heat treatment for 3 hours at 50 °C.

3.5.3 Evaluation of purification effects by SDS-PAGE

For the evaluation of purification effects and to determine whether the same proteins precipitate by spontaneous and heat precipitation SDS-PAGE was used. The results of this analysis are shown in Figure 30.

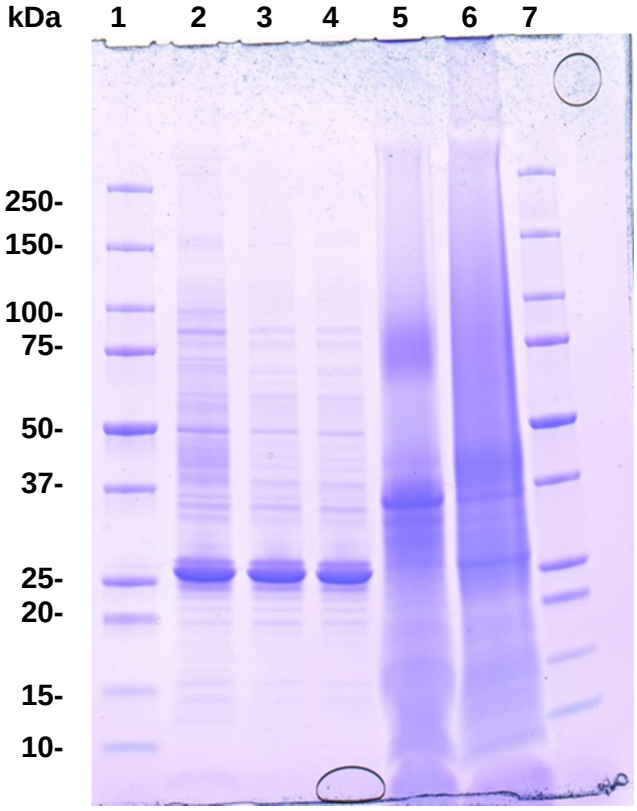

Figure 30:SDS-PAGE gel stained with Coomassie-blue. 1) MW-Std.; 2) Clarified homogenate 25 gCDM/L; 3) Heat precipitated supernatant centrifuged for 15 min.; 4) heat precipitated supernatant centrifuged for 45 min.; 5) Dissolved spontaneously precipitated pellet; 6) Dissolved heat precipitated pellet; 7) MW-Std.

Comparing the clarified homogenate in lane 2 with the heat precipitated homogenate in lane 3 and 4 it is observable that some bands disappeared or got weaker in their appearance, which indicated a lower concentration. Additionally, the smearing along the lanes got weaker, so the quantity of different proteins was reduced. The characteristic band of GFP at approximately 28 kDa did not seem to be affected. The dissolved pellets of spontaneous and heat precipitation looked quite similar, though smearing appears stronger for the heat precipitated pellet and also some additional bands are visible. In the heat precipitated pellet additionally a band at the mass of GFP is visible. There is a significant purification effect by heat precipitation, accompanied by a weak additional precipitation of GFP, which correlates with the results of fluorescence and turbidity measurements.

3.6 Adsorption isotherms

The evaluation of IEX adsorption performance was done by small scale batch adsorption tests. These experiments were used to determine the binding capacity of GFP to the anion exchange resins CaptoQ and Q-Sepharose FF. It was expected to show, if the observed displacement effect is eliminated by different buffer compositions, precipitation and the usage of benzonase. By this means it was possible to determine, if the precipitated compounds or DNA were the reason for the observed displacement effect.

For adsorption isotherms the binding capacity q in mg GFP per mL resin was plotted as a function of the GFP concentration in mg/mL in the supernatant. The binding capacity was

calculated by equation 3.13 where c_0 is the GFP content of the starting material, c_i is the GFP content in the supernatant and V_R is the resin volume. As the used slurry concentration was 50 % resin the used slurry volume had to be divided by two to get the value for V_R.

$$q = \frac{c_0 - c_i}{V_R} \qquad 3.13$$

3.6.1 Heat precipitation

Figure 31 shows the adsorption isotherms for CaptoQ and Q Sepharose FF of clarified and heat precipitated homogenate, the used homogenization buffer for these had a NaCl concentration of 50 mM. Additionally the adsorption isotherms for both resins of a homogenate, homogenized at 60/600 bar for 2 passages, are shown, the used homogenization buffer for these had a NaCl concentration of 100 mM. The used cell suspensions had a cell density of 35 $\frac{\mathrm{gCDM}}{\mathrm{L}}$. For CaptoQ it was observable that the increase of the binding capacity of the clarified homogenate with 50 mM NaCl was steeper than the one of heat precipitated homogenate. Indeed after approximately 2 mg/mL c_i it began to decrease again and went almost to zero for high c_i values. The heat precipitated homogenate's isotherm showed a flatter rise but also a later decrease at approximately 5.5 mg/mL c_i and it did not decrease as much as the clarified homogenate. The maximum binding capacity q_{max} was about 55 mg/mL for both homogenates. The homogenate with a higher salt concentration had an evident lower q_{max} of approximately 17 mg/mL and went to zero at approximately 5 mg/ml supernatant content. For Q-Sepharose FF the maximum binding capacity was about half the level of CaptoQ. Both homogenates with 50 mM NaCl reached a q_{max} of approximately 22 mg/mL for clarified and 25 mg/mL for heat precipitated homogenate, at a c_i of 6 mg/mL. Indeed the clarified homogenate decreased further and reached a final value for q of approximately 13 mg/mL. Whereas the heat precipitated homogenate's value only decreased to 20 mg/mL. At 100 mM NaCl q_{max} reached a value of approximately 10 mg/mL and again reached zero at a c_i of approximately 5 mg/mL.

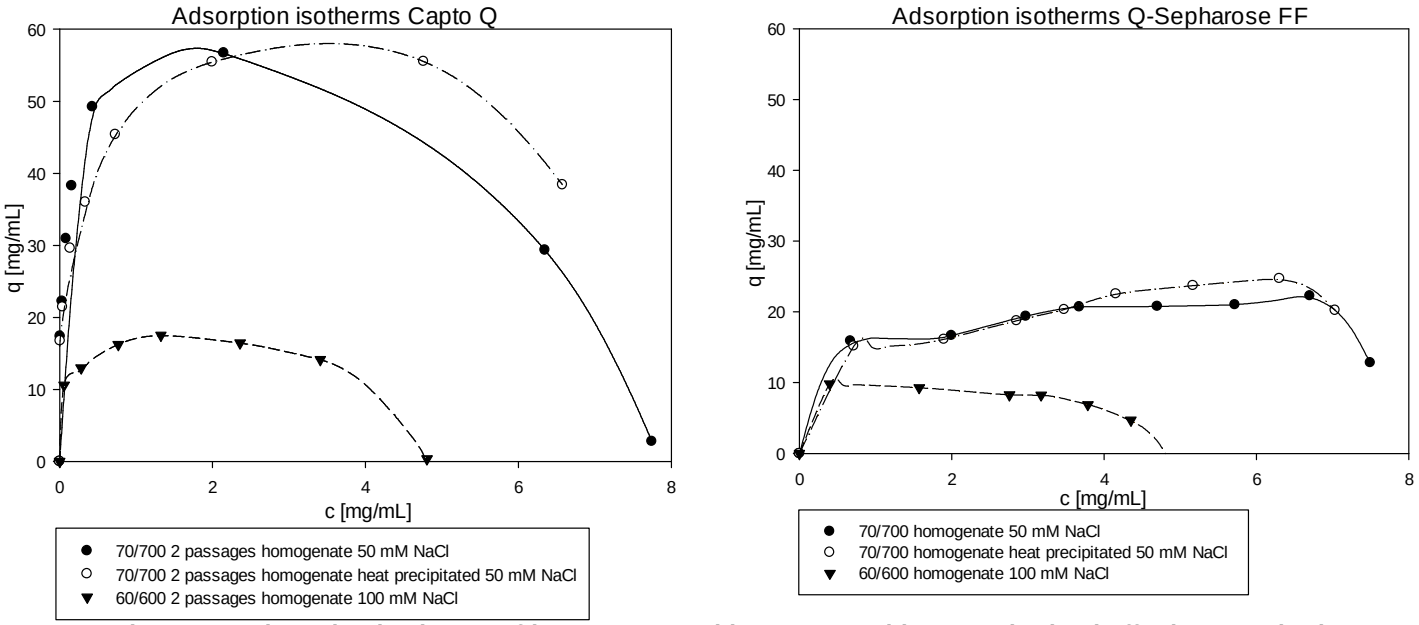

Figure 31: Adsorption isotherms of homogenates with 50 mM NaCl homogenization buffer homogenized at 70/700 bar 2 passages heat precipitated and clarified homogenate, as well as 100 mM NaCl homogenization buffer homogenized at 60/600 bar 2 passages. Used cell suspension had a cell density of 35 gCDM/L. q is the binding capacity in mg GFP per mL resin and c is the GFP content in the supernatant in mg/mL.

The binding capacity of GFP for CaptoQ is evidently higher than for Q-Sepharose FF. Heat precipitation only seems to have little influence on q_{max} but in the case of CaptoQ it shifts the displacement effect to a higher value of c_i so the resin could be loaded with higher amount of GFP. Salt content has a high impact on the binding capacity, half the content results in more than twice the binding capacity.

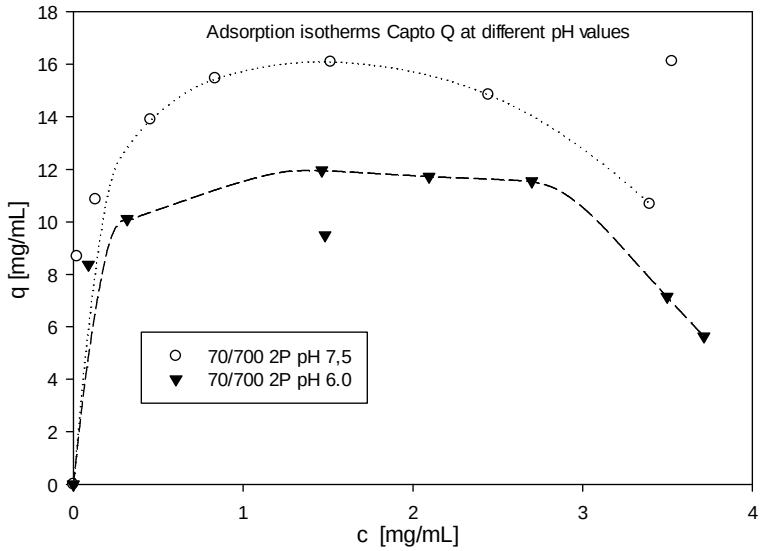

Figure 32: Adsorption isotherms for homogenates of 25 gCDM/L cell suspension in 100 mM NaCl homogenization buffer, homogenized at 70/700 bar for 2 passages. pH values were 7.5 and 6.0. q is the binding capacity in mg GFP per mL resin and c is the GFP content in the supernatant in mg/mL.

Because during the investigations it was detected, that the pH after homogenization decreased to a value of pH 6 it was decided to buffer it up to a pH of 7.5 and determine whether the pH had influence on the adsorption isotherms. The used cell suspension had a cell density of 25 $\frac{\mathrm{gCDM}}{\mathrm{L}}$ and was homogenized at 70/700 bar for two passages. It was observable, that q_{max} at pH 7.5 with a value of approximately 16 mg/mL was higher than at pH 6 with a value of approximately 12 mg/mL. Therefore, at pH 7.5 q_{max} was approximately one third higher than at pH 6. This shows a dependence of the binding capacity on the pH value.

3.6.2 Benzonase treatment

The adsorption isotherms in Figure 33 were performed to show the effect of different homogenization conditions and the treatment of the homogenate with benzonase. The salt content of the homogenization buffer was 100 mM NaCl. Comparing these isotherms with those of Figure 31 confirms the assumption that the higher binding capacity was caused by the lower salt content. Furthermore it lets suggest that homogenization conditions do not have big impact on q as the values are all in the same range. Additionally it seems that the usage of Benzonase does not influence the binding performance.

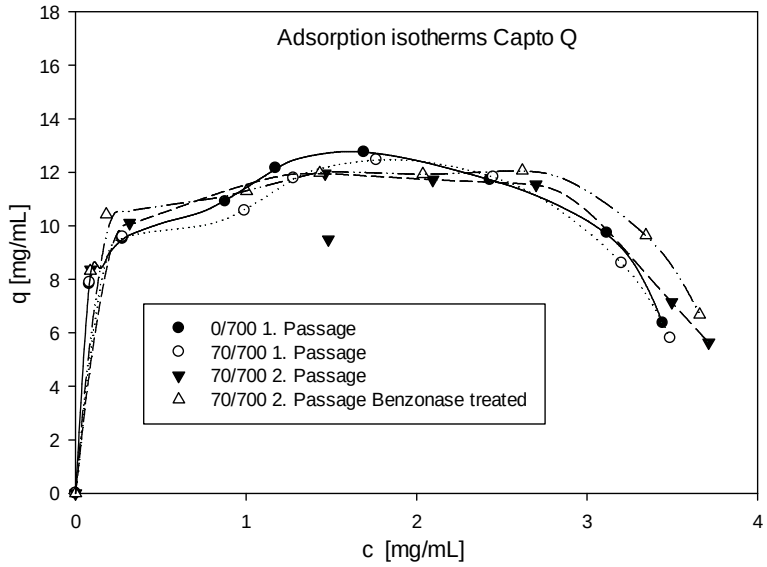

Figure 33: Adsorption isotherms of homogenates of 25 gCDM/L cell suspension in 100 mM NaCl homogenization buffer. Used homogenization conditions were 0/700 bar 1 passage, 70/700 bar 1 passage, 70/700 bar 2 passages and 70/700 2 passages treated with 9 U/mL benzonase. q is the binding capacity in mg GFP per ml resin and c is the GFP content in the supernatant in mg/mL.

In summary, the major influence on the binding capacity during these investigations was observable by salt content. Lower salt content resulted in higher values for q over the entire concentration range. Although heat precipitation had a positive effect on binding performance it was not that high. Another factor that strongly impacts the binding performance is the pH value. If it gets too low q is decreasing strongly. However, benzonase treatment seems not to influence the adsorption. Although the displacement effect was shifted it was not eliminated.

Additionally to the adsorption isotherms, agarose gel electrophoresis was performed to show the fragmentation effect of homogenization and benzonase treatment on DNA. The agarose gel electrophoresis, shown in Figure 34, and the ethanol precipitation correspond quite well. The precipitated DNA is shown in Figure 35. The homogenate of one stage at 700 bar showed bands of high molecular sizes higher than 10.000 bp and approximately 4000 bp. The precipitated DNA of this homogenate formed a kind of filament which is an indication for genomic DNA. After the first passage at 70/700 bar the amount of the bigger fragments was reduced as the band intensity at 10.000 bp decreased, after the second passage no more bands were visible in the upper range and the smear started at lower sizes' range. The benzonase treatment finally cut the fragments into small pieces and the visible band was below 500 bp. Ethanol precipitation also showed that homogenization conditions have impact on the DNA size in the supernatant. A clew only was formed out of the homogenate homogenized with one stage at 700 bar, increasingly harsh homogenization lead to the formation of fine particles which indicate small DNA fragments.

The reason for RNase treatment of the homogenates was that without this treatment massive smearing appeared in the lanes, which is an indication for RNA in the electrophoresis samples.

Summing up the DNA analysis its size depends on homogenization conditions and whether the samples are treated with nucleases. Possibly the fine fragmentation of DNA makes it more difficult to detach it after homogenization and nuclease treatment can solve this problem. Eventually the displacement effects during IEX is caused by these DNA fragments or by RNA which also seems to be present in the samples after cell debris removal but these questions were not examined within this thesis.

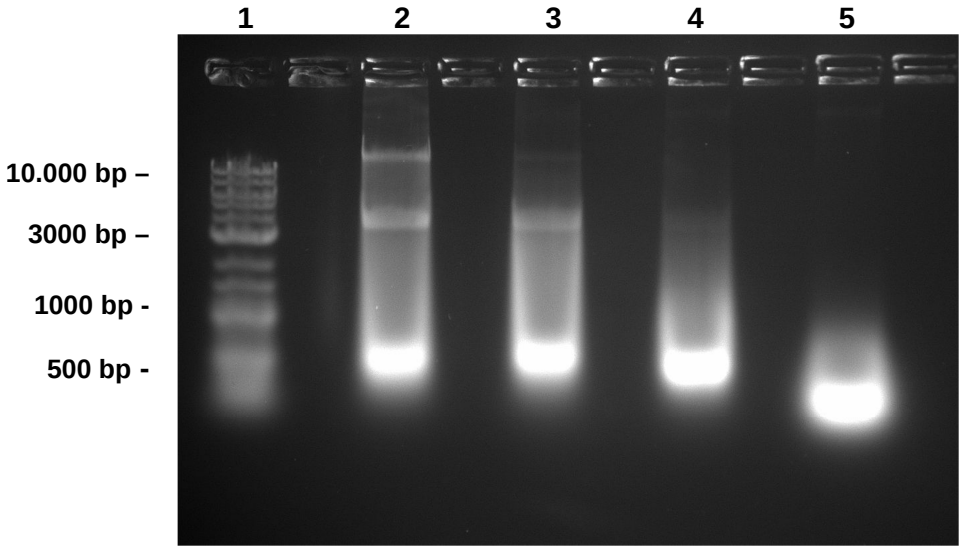

Figure 34: Agarose Gel Electrophoresis gel of differently treated homogenates after RNase treatment. 1) MW Std. 2) 0/700 bar 1. passage; 3) 70/700 bar 1. passage; 4) 70/700 bar 2. pasage; 5) 70/700 bar 2. passage treated with 9 U/mL benzonase.

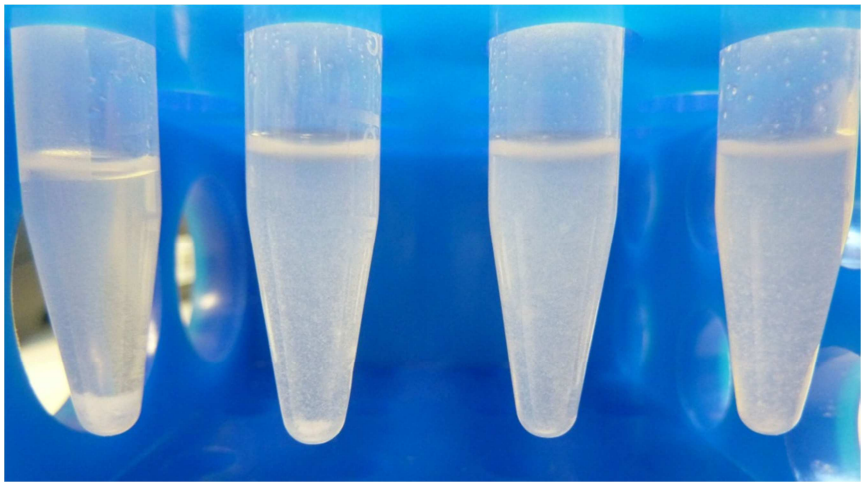

Figure 35: Ethanol precipitated DNA. Samples from left to right: 0/700 bar 1 passage; 70/700 bar 1. passage; 70/700 bar 2. passage; 70/700 bar 2. passage treated with 9 U/mL Benzonase.

4 Summary and conclusion

The precipitation of impurities after centrifugation and filtration was observed during the purification of GFP from *E. coli* fermentation broth. GFP was used as model protein for purification due to its robustness and easy detection.

The precipitate was studied by photometer scans, electrophoresis and protein quantification. These experiments showed that the precipitate mainly consists of protein. The protein masses have a wide variety with a high fraction below 50 kDa. Because for selective precipitation of the impurities the knowledge of conditions that favor spontaneous precipitation was necessary, the impact of homogenization and storage conditions was investigated. It was shown, that on the one hand more precipitate was formed when higher cell densities were homogenized and on the other hand when the homogenate was stored at

higher temperature. According to these results it was decided to use heat as a precipitating agent.

Heat precipitation showed that higher temperature resulted in a higher formation of precipitate but also a higher loss of GFP. For heat precipitation 3 hours at 50 °C was chosen, because high clearance efficiency, a good purification effect and relatively low loss of GFP were accomplished. At 60 °C an exponential relation between GFP content and precipitation time was established. Furthermore, a kinetic for the formation of precipitate was established.

Additionally $CaCl_2$ and PEG were investigated as precipitating agents. These were found of not being capable as purification steps after homogenization as they resulted in too high GFP loss.

The adsorption isotherms showed that homogenization conditions did not influence the binding capacity. Also benzonase treatment did not improve adsorption performance. Heat treatment only shifted the displacement effect to higher feed concentrations but could not eliminate it. A big impact on binding capacity was shown by salt content and pH. Although the reduction of salt content of the homogenization buffer improved the adsorption performance, it is not really favorable to use a homogenization buffer with half the salt content as the effectiveness of heat precipitation decreased.

DNA analysis showed increasing number of stages and passages used for homogenization and the treatment of homogenates with benzonase lead to a size reduction of DNA fragments.

Summing up, heat precipitation seems to be a capable purification step during the downstream processing of *E. coli* fermentation broths.

Concluding, in the course of this thesis it was possible to identify the precipitate and to find a capable unit operation to selectively precipitate these impurities. Furthermore the conditions for precipitation and clearance could be investigated and impacts on the adsorption performance were possible to point out.

Future investigations should deal with the scale up of heat precipitation to use it in pilot scale protein purification. Furthermore, it should be determined if the low impact of heat precipitation on the adsorption performance was caused by the decrease of pH during homogenization and whether the displacement effect is diminished or even eliminated after heat precipitation, if the pH has a higher value. The same applies for the treatment with benzonase. These investigations were already started by Rainer Hahn, Bernhard Sissolak and Sabine Necina and showed quite good results. Additionally the homogenization buffer could be amended insofar as the molarity of Tris is raised for example to the amount that was used by Ng et al. for their heat treatment experiments (Ng et al. 2006). This higher molarity of Tris would lead to a higher buffering capacity and thus may result in a more stable pH value during homogenization and moreover provide the conditions that lead to an improvement of binding capacity.

If these questions are answered, the adsorption kinetics could be subject of further investigations, and may be performed by shallow bed adsorption experiments according to Hahn et al. 2005.

Literature

Alkaabi, K.M., Yafea, A. & Ashraf, S.S., 2005. Effect of pH on thermal- and chemical-induced denaturation of GFP. *Applied biochemistry and biotechnology*, 126(2), pp.149–156.

Bio Rad, Precision Plus Protein Dual Color Standards Instruction manual. , pp.6–8.

Bischof, J.C., 2005. Thermal Stability of Proteins. *Annals of the New York Academy of Sciences*, 1066(1), pp.12–33. Available at: http://doi.wiley.com/10.1196/annals.1363.003.

Blattner, F.R. et al., 1997. The Complete Genome Sequence of Escherichia coli K-12. *Science*, 277(5331), pp.1453–1462. Available at: http://www.sciencemag.org/content/277/5331/1453.short.

Carta, G. & Jungbauer, A., 2010. *Protein Chromatography Process Development and Scale-Up*, WILEY-VCH Verlag GmbH & Co. KGaA.

Doran, P.M., 2013. *Bioprocess Engineering Principles* 2nd Editio., Academic Press.

GE Healthcare, 2015. Capto S, Capto Q, Capto DEAE- Data File. *GE Healthcare Bio-Sciences AB*, pp.1–36. Available at: https://www.gelifesciences.com/gehcls_images/GELS/Related Content/Files/1334667780708/litdoc28407452_20120420103701.pdf.

GE Healthcare, 2004. Ion Exchange Chromatography & Chromatofocusing - Principles and Methods. *GE Healthcare*, pp.1–188.

Giese, G. et al., 2013. Purification of antibodies by precipitating impurities using Polyethylene Glycol to enable a two chromatography step process. *Journal of Chromatography B*, 938, pp.14–21. Available at: http://linkinghub.elsevier.com/retrieve/pii/S1570023213004571.

Hahn, R. et al., 2005. Shallow Bed Adsorption: Theoretical Background and Applications. *Chemical Engineering & Technology*, 28(11), pp.1241–1251. Available at: http://doi.wiley.com/10.1002/ceat.200500221.

Hahn, R. & Luchner, M., 2015. *Bioprocess Engineering Laboratory*,

Jungbauer, A. & Hahn, R., 2008. Polymethacrylate monoliths for preparative and industrial separation of biomolecular assemblies. *Journal of Chromatography A*, 1184(1-2), pp.62–79.

Kelly, W.J. & Muske, K.R., 2004. Optimal operation of high-pressure homogenization for intracellular product recovery. *Bioprocess and Biosystems Engineering*, 27(1), pp.25–37. Available at: http://link.springer.com/10.1007/s00449-004-0378-9.

Nagy, A., 2004. Thermal stability of chemically denatured green fluorescent protein (GFP) A preliminary study. *Thermochimica Acta*, 410(1-2), pp.161–163. Available at: http://linkinghub.elsevier.com/retrieve/pii/S0040603103003976.

Ng, M.Y.T. et al., 2006. Heat treatment of unclarified Escherichia coli homogenate improved the recovery efficiency of recombinant hepatitis B core antigen. *Journal of Virological*

Methods, 137(1), pp.134–139. Available at: http://linkinghub.elsevier.com/retrieve/pii/S0166093406002242.

Novagen, 2003. pET System Manual Novagen. , TB05 10th, pp.1–68.

Overton, T.W., 2014. Recombinant protein production in bacterial hosts. *Drug Discovery Today*, 19(5), pp.590–601. Available at: http://linkinghub.elsevier.com/retrieve/pii/S1359644613004029.

Roda, A., 2010. Discovery and development of the green fluorescent protein, GFP: The 2008 Nobel Prize. *Analytical and Bioanalytical Chemistry*, 396, pp.1619–1622.

Sanders, J.K.M. & Jackson, S.E., 2009. The discovery and development of the green fluorescent protein, GFP. *Chemical Society reviews*, 38(10), pp.2821–2822.

Shimomura, O., 2005. The discovery of aequorin and green fluorescent Protein. *Journal of Microscopy*, 217(January), pp.3–15.

Sommer, R. et al., 2014. Combined polyethylene glycol and CaCl2 precipitation for the capture and purification of recombinant antibodies. *Process Biochemistry*, 49(11), pp.2001–2009. Available at: http://linkinghub.elsevier.com/retrieve/pii/S1359511314003985.

Stone, M.C. & Carta, G., 2007. Patterns of protein adsorption in chromatographic particles visualized by optical microscopy. *Journal of chromatography. A*, 1160(1-2), pp.206–14. Available at: http://www.ncbi.nlm.nih.gov/pubmed/17560582.

Swartz, J.R., 2001. Advances in Escherichia coli production of therapeutic proteins. *Current Opinion in Biotechnology*, 12(2), pp.195–201.

Tsien, R.Y., 1998. The Green Fluorescent Protein. *Annual Reviews of Biochemistry*, 67, pp.509–544.

Vessoni Penna, C. et al., 2004. Thermal Stability of Recombinant Green Fluorescent Protein (GFPuv). *Applied biochemistry and biotechnology*, 113(113-116), pp.469–483.

Wang, D., Merz, T. & van Gunsteren, W.F., 2010. The thermal isomerization of the GFP chromophore: A computational study. *Physical Chemistry Chemical Physics*, 12(36), p.11051. Available at: http://xlink.rsc.org/?DOI=c0cp00181c.

Wong, H.H., O'Neill, B.K. & Middelberg, A.P.J., 1997. A mathematical model for Escherichia coli debris size reduction during high pressure homogenisation based on grinding theory. *Chemical engineering science*, 52(17), pp.2883–2890. Available at: http://www.sciencedirect.com/science/article/pii/S000925099700105X.